

学位論文

Study on novel protein Dsup from an extremotolerant tardigrade, that improves radio-tolerance in human cultured cells

(極限環境耐性をもつクマムシ固有の新規タンパク質 Dsup
によるヒト培養細胞への放射線耐性付与に関する研究)

平成 28 年 6 月 博士（理学）申請

東京大学大学院理学系研究科
生物科学専攻

橋本 拓磨

Contents

Abbreviations.....	3	
Abstract.....	5	
General Introduction.....	7	
 Chapter 1: Dsup protects DNA and improves radio-tolerance in cultured human cells		
Introduction.....	11	
Results.....	13	
Discussion.....	20	
 Chapter 2: Crucial role of DNA-associating C-terminal region in DNA protection and improvements of radio-tolerance by Dsup protein		
Introduction.....	24	
Results.....	25	
Discussion.....	29	
 Conclusion and Future Perspectives.....		32
Materials and Methods.....		36
Figures.....		44
Tables.....		75
References.....		86
Acknowledgements.....		94

Abbreviations

aa, amino acids

BrdU, 5-bromo-2'-deoxyuridine

CAG promoter, Hybrid construct consisting of the cytomegalovirus enhancer fused to the chicken beta-actin promoter

DAPI, 4',6-diamidino-2-phenylindole

dps, days post seeding

Dps, DNA-binding protein from starved cells

DSBs, double-strand breaks

Dsup, damage suppressor

EDTA, ethylenediaminetetraacetic acid

GFP, green fluorescent protein

HEK, human embryonic kidney

H-NS, histone-like nucleoid-structuring protein

MS/MS, tandem mass spectrometry

NAC, N-acetyl-L-cysteine

NLS, nuclear localization signal

PBS, phosphate-buffered saline

PCR, polymerase chain reaction

pI, isoelectric point

PI, propidium iodide

RFU, relative fluorescence units

ROS, reactive oxygen species

RT, room temperature

S2, *Drosophila* schneider 2

SASP, small acid-soluble spore protein

shRNA, small hairpin RNA

SSBs, single-strand breaks

TBE, tris-borate-EDTA

wt, weight

Abstract

High dose radiation severely damages DNA and other essential molecules leading most organisms to death. However, some organisms possess extraordinary tolerance against radiation. Tardigrades, also known as water bears, are small aquatic animals. Some tardigrade species can tolerate almost complete dehydration and exhibit tolerance to various physical extremes in the dehydrated state. *Ramazzottius varieornatus* is one of the most stress-tolerant tardigrade species that survives 4,000 Gy ^4He -ion irradiation even in a hydrated state. There should be efficient mechanisms to protect DNA from radiation and/or repair radiation-induced DNA damages in the organism, but the molecular mechanisms enabling the exceptional radiation resistance remain totally unknown. As a candidate protein involved in the radiation tolerance, I focused on a novel DNA-associating protein, termed S261 (I renamed this protein ‘Damage suppressor’ (Dsup) after functional analysis in this study. Hereafter, I refer to this protein as Dsup), identified from a chromatin fraction of *R. varieornatus* in the former study in our laboratory (Y. Saito, master’s thesis). Dsup exhibits no sequence similarity with any known proteins or motifs, and localizes around nuclear DNA in insect cells. Here, I show that Dsup protein has a nuclear localization signal and also localizes around nuclear DNA in tardigrade cells and in transfected human cultured cells. Stable expression of Dsup protein in human cultured cells significantly suppressed DNA fragmentation and DNA breaks caused by X-ray irradiation or reactive oxygen species. Furthermore, after 4 Gy X-ray irradiation, some fraction of Dsup-expressing cells survived and even retained proliferative ability, whereas no proliferation was observed in untransfected cells. Knockdown of *Dsup* using shRNA completely abolished the DNA protection and improved survival after irradiation. These findings indicate that Dsup protects

DNA from radiation-induced damage and provides a novel and promising means to improve radiation resistance of intolerant animal cells. Next, I examined whether the association between Dsup protein and DNA is important for these protection activity. In my master course studies, I showed that C-terminal region is necessary and sufficient for localization of Dsup protein around nuclear DNA. Based on these findings, in my doctoral course study, I established a cell line stably expressing the mutant Dsup protein, Dsup Δ C, lacking the C-terminal DNA-associating region, and confirmed that Dsup Δ C protein localized mainly in the cytoplasm. In contrast to the full-length Dsup-expressing cells, the Dsup Δ C-expressing cells exhibited no reduction in the DNA fragmentation compared to HEK293 cells in alkaline comet assays, suggesting that the association with DNA is prerequisite for Dsup to protect DNA from single-strand breaks. Furthermore, in the assay detecting DNA double-strand breaks utilizing gamma-H2AX foci as an indicator, the Dsup Δ C-expressing cells exhibited the impaired reduction of DNA double-strand breaks compared to the full-length Dsup-expressing cells, further supporting the importance of the association with DNA in the DNA protection activity of Dsup protein. This is the first report to my knowledge that introduction of a DNA-associating protein from an extremotolerant animal into human cultured cells confers DNA protection from radiation and improves the survival and proliferative ability of irradiated cells.

General Introduction

For all organisms, proper maintenance of genomic DNA is critical for preserving correct genetic information and normal cellular functions. Genomic DNA is constantly attacked by various genotoxic agents of both intrinsic and extrinsic origin, e.g., metabolically generated reactive oxygen species (ROS) or radiation exposure [Jackson, S. P. (2002); Ciccia, A. *et al.* (2010)]. Organisms employ multiple mechanisms to combat these damaging agents, including various DNA repair processes and detoxification of the causative agents. In most organisms, including humans, however, the tolerable capacity is limited and excessive genotoxic stress such as high-dose radiation, causes severe DNA lesions including double-strand breaks (DSBs), and leads to loss of proliferative ability or even death [Ward, J. F. (1994); Jackson, S. P. *et al.* (2009); Chapman, J. R. *et al.* (2012)]. This limitation prevents these organisms from advancing to genotoxic environments; e.g., space radiation remains major hazard for humans advancing to Mars [Cucinotta, F. A. *et al.* (2013)]. In contrast, some organisms exhibit extraordinary tolerance to radiation.

Tardigrades, also known as water bears, are tiny aquatic animals having four pairs of legs (~0.1-1.2 mm body length). More than 1,000 species have been reported from various habitats, such as marine, fresh-water, or limno-terrestrial environments. Some terrestrial tardigrades species, such as *Ramazzottius varieornatus* and *Milnesium tardigradum*, are typical animals exhibiting an exceptional radio-tolerance. These tardigrades are reported to survive even after exposure to irradiation with 4,000 – 6,000 Gy of gamma-rays or more hazardous He-ion beams [Horikawa, D. D. *et al.* (2006; 2008)], whereas 2 to 10 Gy of gamma-rays is near a median lethal dose for human cells [John, E. B. (1981); Noda, A. *et al.* (2012)]. The molecular mechanisms enabling the exceptional radio-resistance in tardigrades, however, remain unknown.

At present, the most studied radio-resistant organism is the bacterium *Deinococcus radiodurans*. *D. radiodurans* tolerates irradiation with 5,000 Gy of gamma-rays without loss of viability [Battista, J. R. (1997)]. Irradiated *D. radiodurans* presents with severe fragmentation of its genomic DNA, but their fragmented DNA is rapidly patched up to complete circular genome by extensive DNA repair processes [Zahradka, K. *et al.* (2006)]. Mutation of DNA repair pathways drastically compromises the radio-tolerance of *D. radiodurans*, suggesting that their high radio-resistant ability depends on powerful DNA repair processes [Slade, D. *et al.* (2011)]. In other animals as well, DNA repair processes are supposed to be important for extraordinary radio-tolerance, although the exact repair mechanisms remain unknown in radio-tolerant animals having large genomic DNA with chromatin structures. Bdelloid rotifers exhibit extraordinary resistance against ionizing radiation [Gladyshev, E. *et al.* (2008)]. Although they show severe DNA breaks after irradiation at a similar level to radio-intolerant species, such as mammalian cells [Gladyshev, E. *et al.* (2008)], they have the ability to reassemble the fragmented DNA [Hespeels, B. *et al.* (2014)]. Bdelloid rotifers possess high anti-oxidant activity, which is suggested to protect the repair machinery from radiation damage, possibly enhancing DNA repair processes [Krisko, A. *et al.* (2012)]. Both *D. radiodurans* and bdelloid rotifers tolerate severe dehydration as well as radiation. Radiation tolerance of these organisms is proposed to be an evolutionary consequence of adaptation to desiccation stress, because dehydration, like radiation stress, causes DNA damage, and desiccation is a more common environmental stress to terrestrial organisms than radiation. The sleeping chironomid *Polypedilum vanderplanki* is also resistant to dehydration and radiation. Dehydration leads to severe DNA breaks in *P. vanderplanki*, with as much as 40% to 50% of the DNA fragmented [Gusev, O. *et al.* (2010)]. The fragmentation damage is comparable to that induced by irradiation with a 70-Gy He-ion beam, but is subsequently effectively repaired [Gusev, O. *et al.* (2010)]. In contrast, the

radio-tolerant tardigrade *Milnesium tardigradum*, which is resistant to dehydration as well as radiation, has much fewer DNA breaks after dehydration stress, with only approximately 2% of DNA detected as fragmented after 2 days dehydration [Neumann, S. *et al.* (2009)]. DNA in tardigrades seems to suffer much less damage by dehydration stress compared to other organisms [Neumann, S. *et al.* (2009); Rebecchi, L. *et al.* (2009)]. These observations led me to postulate the existence of mechanisms in tardigrades that protect DNA from damaging agents and that such mechanisms contribute to the extreme radio-tolerance of the animals.

In this study, I focused on a novel DNA-associating protein termed Dsup identified from the chromatin fraction of the radio-tolerant tardigrade, *Ramazzottius varieornatus*. I analyzed the localization of Dsup protein in tardigrade cells and human cultured cells. Then, I examined whether Dsup-expressing cells exhibit DNA protection from X-ray irradiation *in vivo*. Furthermore, I examined whether which region of Dsup protein is important for the DNA protection activity. These findings lead to the identification of a novel DNA-protecting protein, and I propose a novel mechanism for conferring improved radio-tolerance to sensitive cells through protection of DNA.

Chapter 1

**Dsup protects DNA protection and improves
radio-tolerance in cultured human cells**

Introduction

High-dose radiation causes severe DNA damage and lethal effects. The tardigrade *Ramazzottius varieornatus* (Figure 1) is an extraordinarily radiation-resistant animal that can survive even 4,000 Gy ^4He -ion irradiation by unknown mechanisms [Horikawa, D. D. *et al.* (2008)]. Considering DNA as a major target of radiation damage, I postulated that putative protection proteins exist around the DNA in the tardigrade. Mr. Yuki Saito, a former master course student in our laboratory, isolated the chromatin fraction from the tardigrade and utilized tandem mass (MS/MS) spectrometry to identify the proteins selectively contained in the chromatin fraction [Hashimoto, T. *et al.* in press]. Among the identified proteins, Y. Saito examined subcellular localization of putative nuclear proteins by expressing them as green fluorescent protein (GFP)-fused proteins in *Drosophila* Schneider 2 (S2) cells. Among them, one protein, that Y. Saito termed S261 (I renamed this protein ‘Damage suppressor’ (Dsup) after functional analysis in this study. Hereafter, I refer to this protein as Dsup), localized around nuclear DNA, whereas the others showed spotted localization in the nuclei without overlapping with DNA localization. The amino acid sequence of Dsup protein (445 amino acids) (Figure 2) showed no similarity to any proteins or motifs in BLASTP and InterProScan searches, suggesting that this protein is novel and unique to the tardigrade. As the isoelectric point is highly basic (pI = 10.55), it is plausible that Dsup directly interacts with DNA. Considering that there are no similar genes in other phyla, Dsup is a good candidate protein involved in the exceptional mechanisms in tardigrades, for protection or repair of DNA upon irradiation.

In this chapter, as a candidate molecule involved in protection of radiation-induced DNA damages, I analyzed properties and the function of Dsup protein *in vivo*. To verify the localization of Dsup protein in tardigrade cells, I performed immunohistochemistry with

frozen sections of tardigrade embryos. To examine functional properties of Dsup, I also investigated the localization of Dsup in human cultured cells in which various gene-manipulation techniques are applicable. I created a stable Dsup-expressing human cultured cell line, and examined whether Dsup protein is involved in DNA protection from X-ray irradiation or reactive oxygen species as a DNA damage inducer *in vivo*. Furthermore, I analyzed whether the expression of Dsup protein improves the survival of irradiated cells.

Results

Dsup protein localized around nuclear DNA in animal cells.

GFP-fused Dsup protein exhibits localization around nuclear DNA in *Drosophila* S2 cells (master course thesis of Y. Saito). In my master course studies, to verify the localization of Dsup protein in tardigrade cells, I raised antibody against Dsup and performed immunohistochemistry using frozen sections of tardigrade embryos with affinity-purified Anti-Dsup antibody. In almost all tardigrade cells expressing Dsup, Dsup protein was detected around nuclear DNA (Figure 3). The transcriptome data revealed abundant expression of Dsup in an early embryonic stage (FPKM > 800; within the top 100 abundantly expressed genes) [Hashimoto, T. *et al.* in press], which is consistent with my immunohistochemistry results, because nuclear DNA rapidly replicates in the embryonic stage. Since reverse genetic methods were limited and a method of primary culture was not established in tardigrades, I utilized human cultured cells, which are easy to apply genetic manipulation, to examine functional properties of Dsup. I first examined localization of Dsup overexpressed in human cultured HEK 293T cells. Dsup-GFP fusion proteins transiently expressed in HEK293T cells localized around nuclear DNA (Figure 4), suggesting that association of Dsup proteins with nuclear DNA is common in both tardigrade and human cells.

DNA electrophoretic mobility shift assay of Dsup protein.

Although Dsup protein showed no sequence similarity to any proteins or motifs in BLASTP and InterProScan searches, it is highly basic (isoelectric point, pI = 10.55), suggesting its potential association with DNA through electrostatic interactions. To examine the association of Dsup protein to DNA, I performed a gel shift assay using bacterially expressed Dsup

protein *in vitro*. Pre-incubation with purified Dsup protein significantly retarded the migration of linearized plasmid DNA in a dose dependent manner (Figure 5), indicating that Dsup protein has ability to associate with DNA. When Dsup protein was mixed with DNA at a 10:1 (wt:wt) ratio, the migration of DNA was almost completely inhibited. A similar drastic change in the band shift was observed in a dose-dependent manner, when I used the ubiquitous chromatin protein mammalian histone H1 (Figure 5), suggesting that Dsup proteins formed huge complexes with DNA and/or neutralized the negative charge of the DNA when enough proteins were available, like histone H1. The higher protein:DNA ratio, however, was required for a complete band shift with Dsup protein compared to histone H1 (Figure 5), suggesting relatively weak DNA associating activity of Dsup compared to histone H1.

Dsup protein suppressed X-ray and reactive oxygen species induced single-strand breaks in human cultured cells.

I hypothesized that the association of Dsup proteins with nuclear DNA might help to protect DNA from irradiation stress. To test this possibility, I tried to establish a HEK293 cell line stably expressing Dsup under the control of the constitutive CAG promoter. Among the clones established, those that showed abnormal morphology were discarded. I also excluded clones that showed non-nuclear localization of Dsup protein in immunocytochemistry. Finally, I selected one clone expressing the highest level of Dsup protein with nuclear localization in immunocytochemistry (Figure 6).

X-ray irradiation induces various types of DNA damage, including DNA strand breaks, mainly single-strand breaks. To examine the effect of Dsup on X-ray irradiation induced DNA strand breaks, Dsup-expressing cells and untransfected HEK293 cells were exposed to 10 Gy X-ray irradiation. After irradiation, the cells were exposed to an alkaline

condition ($\text{pH} > 13$) to denature the damaged DNA, and the resulting dissociated single-strand DNA fragments were analyzed in single-cell electrophoresis (alkaline ‘comet assay’). In this assay, more shortly fragmented DNA migrate to more distant location from the nuclei, forming the ‘comet tail’ region, and thus the proportion of DNA contained in the ‘comet tail’ is considered an indicator of DNA strand breaks. In untransfected HEK293 cells, the proportion of DNA contained in the comet tail increased to 33% after the X-ray irradiation (Figure 7a, Table 1 and 2). In irradiated Dsup-expressing cells, the proportion of DNA contained in the ‘comet tail’ was 16%, which was less than half of that in the untransfected HEK293 cells (Figure 7a). This finding suggested that Dsup protein suppressed X-ray induced single-strand breaks (SSBs) in human cultured cells.

X-ray irradiation induces SSBs through two modes of action: direct effects and indirect effects [Biaglow, J. E. *et al.* (1981)]. Direct effects are attributed to the direct absorption of X-ray energy into the DNA, while indirect effects are caused by the generation of reactive oxygen species (ROS) from water molecules activated by X-ray energy. Therefore, I next used hydrogen peroxide instead of X-rays to examine whether Dsup protein could also protect DNA from ROS. Exposure to hydrogen peroxide induced severe fragmentation of DNA in control HEK293 cells, and 71% of the total DNA was contained in the comet tail. In contrast, DNA fragmentation was substantially suppressed in Dsup-expressing cells and only 18% of the total DNA was contained in the comet tail (Figure 7b, Table 3 and 4), indicating that Dsup protein was able to protect DNA not only from X-rays but also from ROS. Pretreatment with anti-oxidant N-acetyl-L-cysteine (NAC) also substantially suppressed hydrogen peroxide induced SSBs. The combination of NAC and Dsup exhibited even better suppression, though the suppression in combination did not reach a sum of those in each treatment (Figure 7b), suggesting that NAC and Dsup shared common suppression mechanisms at least partially, most likely counteraction to oxidative stress.

Dsup protein reduced DNA double-strand breaks caused by X-ray.

Besides SSBs, high-dose X-ray irradiation also induces double-strand breaks (DSBs), which are much more hazardous for organisms due to the difficulty to repair. Therefore, I next examined whether Dsup protein can also protect DNA from DSBs, by using a neutral comet assay, in which DNA of irradiated cells were analyzed in a neutral condition, without dissociating the duplex DNA into single-strand DNA, which allows to detect only DSB-generated DNA fragments. In untransfected cells, X-ray irradiation increased the proportion of fragmented DNA from 8 to 36% (Figure 7c, Table 5). In contrast, in Dsup-expressing cells, although DNA fragmentation also increased from 6 to 21% by X-ray irradiation, the proportion of fragmented DNA was reduced by approximately 40% (from 36% to 21%) compared to that in untransfected cells (Figure 7c, Table 5 and 6). These findings suggest that Dsup protein suppressed X-ray induced DNA DSBs as well as SSBs.

I further verified the suppression of DNA damage by Dsup proteins using another DSB quantification method. In irradiated cells, histone H2AX around DSBs becomes phosphorylated within an hour after irradiation, which is referred to as γ -H2AX, and thus γ -H2AX can be used as an indicator of DSBs. I visualized γ -H2AX by immunocytochemistry and counted the number of foci per nucleus at 1 h after irradiation. For this experiment, I irradiated cells with a relatively lower dose (1 Gy) of X-ray to avoid overlap of multiple foci and minimize corresponding counting errors. In Dsup-expressing cells, the number of γ -H2AX foci decreased by approximately 40% compared to untransfected cells (Figure 8a, Table 7 and 8), further supporting that Dsup protein suppressed X-ray induced DNA DSBs.

Next, to confirm that suppression of DNA damage in Dsup-expressing cells actually depends on Dsup protein expression, I transfected an expression construct of a small hairpin RNA (shRNA) targeting Dsup into Dsup-expressing cells to generate *Dsup*

knockdown cells. shRNA transfection successfully reduced *Dsup* expression by 77% (Figure 8b). The number of foci in irradiated *Dsup* knockdown cells was similar to that in untransfected (non-*Dsup*-expressing) HEK293 cells (Figure 8c, d, Table 7 and 9) and suppression of DNA damage was completely abolished by *Dsup* knockdown. These findings clearly indicated that *Dsup* protein is responsible for the suppression of DNA damage in irradiated human cultured cells.

***Dsup* protein improved cell viability and proliferative ability of irradiated human cells.**

Generally, 3 to 7 Gy of X-ray induces severe DNA damage in mammalian cells, leading to loss of proliferative ability [Puck, T. T. *et al.* (1956)]. The observed DNA protection in *Dsup*-expressing cells prompted me to hypothesize that *Dsup* could also improve cellular survival after irradiation. To examine this possibility, I measured the cell viability after irradiation. I irradiated cells with 4 Gy X-ray at 1 day post seeding (dps), that was the minimum dose enough to suppress proliferation of untransfected HEK293 cells in this condition. After irradiation, cell proliferation was measured at 24-h intervals using PrestoBlue Cell Viability reagent, which measures the total reducing power of the cell culture [Xu, M. *et al.* (2015)]. In untransfected HEK293 cells, cell proliferation almost ceased at 1 d after irradiation (2 dps), and the total cell viability was maintained at the similar level till 8 dps (Figure 9b). In contrast, irradiated *Dsup*-expressing cells exhibited continuously increasing total cell viability to seven-fold at 8 dps (Figure 9b). Because *Dsup*-expressing cells exhibited slightly faster proliferation under non-irradiated conditions (Figure 9a), I compared cell viability after normalizing the viability of irradiated *Dsup*-expressing cells with that of non-irradiated *Dsup*-expressing cells, and confirmed that *Dsup*-expressing cells exhibited slightly better survival than untransfected cells under irradiated conditions at 4 dps (Figure 9c). After the cell viability analysis, I performed phase contrast microscopy to

analyze the morphology of irradiated cells at 12 dps and observed drastic differences between Dsup-expressing cells and untransfected cells (Figure 9d). Almost all irradiated untransfected cells had an abnormal round shape and were detached from the bottom of the culture dish, which are typical characteristics of the dead cells. In contrast, many irradiated Dsup-expressing cells had a normal morphology and attached to the bottom of culture dishes, which are characteristics of live adherent cells and consistent with the notion that irradiated Dsup-expressing cells had proliferative ability.

To confirm that Dsup-expressing cells actually had proliferative ability even after irradiation, I examined the temporal change of cell numbers after irradiation with 4 Gy of X-ray over a longer period. Under non-irradiated conditions, Dsup-expressing cells proliferated slightly faster than the untransfected cells, which was consistent with my previous observation, whereas *Dsup*-knockdown cells exhibited similar proliferation to that of untransfected cells (Figure 10b and Table 10). At 10 to 12 dps, the cell numbers became nearly saturated. Under irradiated conditions, phase contrast microscopy revealed that almost all untransfected cells detached from the culture dish and had an abnormal round shape morphology like dead cells, consistently from 8 to 12 dps (Figure 10a). In contrast, some of the irradiated Dsup-expressing cells attached to the bottom of the culture dish with an apparently normal morphology and the number of such cells increased over times (Figure 10a). Cell counting analyses confirmed these observations. At 8 dps, the number of irradiated untransfected cells did not change significantly from that at 0 dps and subsequently decreased at 10 and 12 dps (Figure 10b and Table 10). In contrast, the number of Dsup-expressing cells increased even at 8 dps compared to that at 0 dps, and drastically increased at 10 and 12 dps (Figure 10b and Table 10), suggesting that at least some fraction of irradiated Dsup-expressing cells retained the proliferative ability. Growth rates of irradiated Dsup-expressing cells at 8 to 12 dps were almost comparable to those of non-irradiated

Dsup-expressing cells. In *Dsup*-knockdown cells, the improvements in cell viability and proliferative ability were completely abolished and their phenotypes were similar to those of untransfected HEK293 cells (Figure 10). In addition, because radio-sensitivity of mammalian cells is affected by the cell cycle, I examined whether Dsup protein expression altered the cell cycle distribution. Cells were classified to each cell cycle phase based on DNA content and incorporation of pulse-labeled BrdU using flow cytometer. No significant differences in the distribution of the cell cycle were detected between Dsup-expressing cells and untransfected HEK293 cells (Figure 11a, b), indicating that the improved radio-tolerance conferred by Dsup protein was not due to alterations of the cell cycle. Taken together, these findings strongly suggested that Dsup expression improved cell viability and even the proliferative ability of irradiated human cultured cells and Dsup protein conferred increased radio-tolerance upon human cultured cells.

Discussion

In this chapter, I analyzed functional properties of a novel DNA-associating protein, Dsup, from a radio-tolerant animal, *R. varieornatus*. Dsup protein exhibited an association with DNA *in vitro* and protected DNA in human cultured cells from both X-ray irradiation and hydrogen peroxide. Furthermore, some fraction of Dsup-expressing human cultured cells survived and even retained their proliferative ability after 4 Gy X-ray irradiation, which completely suppressed the growth of untransfected cells.

Although Dsup protein was essentially detected in nuclei in tardigrade embryos, I could not detect Dsup expression in some population of embryonic cells (Figure 3). According to transcriptome data, the expression of Dsup was maintained at high level throughout embryogenesis and I speculate that some embryonic cells might express Dsup at later stages and not all cells express Dsup in mid-embryonic stage when the subcellular localization was examined in this study. In *R. varieornatus*, embryo was reported to exhibit relatively low radio-tolerance ($LD_{50} \sim 500$ Gy) when compared with adult [Horikawa D. D. *et al.* (2012)]. Partial or low accumulation of Dsup protein in some embryonic cells might be attributed to a relatively weak radio-tolerance in embryonic stage. In immunohistochemistry, weak signals were also detected at the surface of embryonic tardigrade, possibly due to non-specific binding of IgGs to the egg-shells (Figure 3).

I detected ~ 40 foci of γ -H2AX (Figure 8a,c), which is relatively high when compared with those in preceding reports [Rothkamm, K. *et al.* (2003); Burg, M. *et al.* (2006)], in untransfected HEK 293 cells at 1 h after 1 Gy irradiation on the glass coverslips. Irradiated glass materials are reported to enhance the irradiation effects approximately twice by generating the secondary electrons [Kegel, P., *et al.* (2007)]. Taking this effect into account, the detected number of γ -H2AX in this assay seems well concordant with the

previous reports, in which 20~30 DSBs were detected after 1 Gy irradiation [Rothkamm, K. *et al.* (2003); Burg, M. *et al.* (2006)].

Mobility shift assay suggested the association of Dsup protein with DNA and I propose that this property attributed to the improved DNA protection in Dsup-expressing cells, which was examined by using ‘comet assays’ (Figure 7). The suppression of fragmented DNA migration in Dsup-expressing cells was observed even in alkaline comet assay, in which the cells were lysed and electrophoresed under the strong alkaline condition ($\text{pH} > 13$). Under this condition, most proteins are assumed to be denatured to lose their molecular activities, and therefore I speculate that it is unlikely that Dsup protein still affected DNA mobility in alkaline comet assay; for example, by binding together the fragmented DNAs. However, as Dsup protein is a novel protein, I can not definitely exclude the possibility that Dsup protein is highly resistant to denaturing alkaline conditions and retains the associating capacity to DNA even in pH higher than 13. To test this possibility, it might be effective to examine whether Dsup protein could still bind to DNA in mobility shift assay under alkaline condition.

In my comet assays, Dsup-expressing cells were irradiated on ice (Figure 7a,c) or treated with hydrogen peroxide at 4°C (Figure 7b), and immediately subjected to electrophoresis, suggesting that DNA fragmentation was detected prior to significant DNA repair. In the γ -H2AX foci assay, I detected γ -H2AX foci at 1 h after irradiation when enough γ -H2AX has accumulated to be detected in human cells, and the accumulation of γ -H2AX is normally retained for at least several hours [Taneja, N. *et al.* (2004); Andrievski, A. *et al.* (2009); Noda, A. *et al.* (2012)]. Thus, I concluded that the reduced number of DNA breaks in Dsup-expressing cells was due to the suppression of DNA breaks, rather than facilitation of DNA repair processes, which is proposed in some other radio-tolerant animals, such as the sleeping chironomid or rotifers [Gusev, O. *et al.* (2010); Krisko, A. *et al.* (2012)]. In some

desiccation-tolerant animals, protective molecules, such as trehalose, are thought to play important roles in the protection of biomolecules against dehydration stress. Dsup could be a DNA-targeted protectant in the tardigrade, though this finding would not exclude the possibility of the presence of an effective DNA repair system.

Dsup protected DNA from a hydrogen peroxide treatment as well as X-ray irradiation (Figure 7b). This suggests that Dsup protein could protect DNA from the indirectly generated ROS when irradiated with X-ray. Although the precise mechanisms of DNA protection by Dsup remain to be elucidated, Dsup protein could interfere attack by ROS to DNA.

Strikingly, some fraction of Dsup-expressing cells retained their proliferative ability even after irradiation with lethal dose of X-rays (Figure 9 and 10). Proliferative survivor cells were morphologically normal. What type of cells can survive irradiation with the aid of Dsup protein? In irradiated Dsup-expressing cells, the extent of the DNA damage varied among cells, and some fraction of cells suffered much less damage than other cells. In cells incurring a correctable amount of DNA damage, the damage might be almost completely repaired, allowing the cells to proliferate even after a lethal dose of X-ray irradiation. Although radio-sensitivity varies depending on the cell cycle [Sinclair, W. *et al.* (1966)], the Dsup-expressing cells exhibited no alteration in the distribution of cell cycle compared to HEK293 cells. This suggested that the improved radio-tolerance conferred by Dsup protein could be attained by novel mechanisms other than alteration of the cell cycles. These findings provide novel insights into the radio-tolerant mechanisms in animal cells that protect genomic DNA with chromatin structures.

Chapter 2

Crucial role of DNA-associating C-terminal region in DNA protection and improvements of radio-tolerance by Dsup protein

Introduction

In Chapter 1, I showed that Dsup proteins are localized around nuclear DNA in both human cultured HEK293T cells and tardigrade cells. Dsup protein has an ability to associate with DNA *in vitro*, suggesting that its localization around nuclear DNA in the cells is due to the association to DNA. I also revealed that introduction of Dsup protein significantly suppressed DNA damage in irradiated human cultured cells. Furthermore, expression of Dsup protein significantly improved the survival of irradiated cells and some fraction of cells retained their proliferative ability even after 4 Gy X-ray irradiation. Based on these findings, I concluded that Dsup protein confers radio-tolerance to human cultured cells. However, it is unknown what kind of molecular characteristics of Dsup are attributed to its subcellular localization and ability to improve radio-resistance, since Dsup protein showed no sequence similarity to any known proteins or motifs. In this chapter, I analyzed whether which region of Dsup protein is important for the nuclear localization and DNA protection.

At first, to search for novel motif structures of Dsup, I performed the secondary structure prediction *in silico* based on its amino acid sequence. I found that Dsup protein can be divided into three regions, N-terminal region, the middle α -helix region and C-terminal region. To examine the role of each region for nuclear localization, I generated various Dsup mutants lacking the N-terminal region, α -helical region and C-terminal region, respectively. Then, I examined whether which region of Dsup protein is important for the ability to associate with DNA and also for DNA protection. The results indicated that the C-terminal region has crucial roles in both abilities of Dsup protein to associate with DNA and to protect DNA.

Results

***In silico* analysis of Dsup protein.**

Dsup protein showed no sequence similarity to any known proteins or motifs in BLASTP and InterProScan searches. In my master course studies, to reveal a novel motif structure of Dsup, I performed the secondary structure prediction based on its amino acid sequence. *In silico* prediction revealed a putative long α -helical structure in the middle region of the protein (142-206 aa) (Figure 12). The putative helical structure has amphiphilic characteristics and I postulated that this region might be involved in protein-protein interaction via hydrophobic interaction. I also found a putative nuclear localization signal (NLS) at the C-terminus (Figure 12). This suggests that C-terminal region might be crucial for the nuclear translocation.

Dsup protein is highly basic (pI = 10.55). In my doctoral course study, to reveal especially basic regions in Dsup protein, I analyzed the distribution of basic amino acid residues by drawing a charge plot, and the plot indicated that the C-terminal region is highly basic (Figure 12). A highly basic (positively charged) region tends to associate with negatively charged nucleic acid. Thus, the C-terminal region could be involved in association with DNA through electrostatic interactions. Based on these results, I divided Dsup protein into three regions, the N-terminal region, the middle α -helix region and the C-terminal region.

C-Terminal region is responsible for localization to nuclear DNA.

To identify the region responsible for the nuclear translocation and localization of Dsup protein around nuclear DNA, I introduced variously deleted mutant Dsup proteins that are

fused with GFP into HEK293T cells and examined their subcellular localization. Deletions of the N-terminal region (Dsup Δ N) or the middle α -helix region (Dsup $\Delta\alpha$ H) did not affect the localization of Dsup-GFP fusion proteins (Figure 13a). In contrast, mutant protein lacking the C-terminal region (Dsup Δ C) was exclusively localized in the cytoplasm and no significant protein was detected in the nucleus (Figure 13a). These findings indicated that the C-terminal region was essential for the nuclear localization of Dsup protein, which is consistent with the fact that a NLS is predicted at the C-terminus (Figure 12). In addition, I examined whether the C-terminal region alone (Dsup-C) was sufficient for nuclear localization, and found that Dsup-C-GFP fusion protein is also localized in the nucleus and even around nuclear DNA (Figure 13c), indicating that the C-terminal region was responsible for localization of the Dsup protein near nuclear DNA. To narrow down the region responsible for the nuclear translocation and localization around nuclear DNA, I generated further Dsup-C deletion derivatives and examined their localization in HEK293T cells expressing these mutant proteins fused with GFP. The C-terminal fragment that comprises 93 amino acid residues including the putative NLS was sufficient for translocation to nucleus, whereas the translocation to nucleus gradually diminished with further deletions (Figure 13c). Interestingly, expression of Dsup-C induced an abnormal aggregation of nuclear DNA, whereas full-length Dsup-expressing cells exhibited no significant alteration in distribution of nuclear DNA compared to that in control cells (Figure 13b, c). These results suggested that without the N-terminal and α -helix regions, the Dsup-C associates too tightly with DNA, which might affect the higher order structure of chromatin and DNA.

Dsup protein associates with DNA through the C-terminal region.

Dsup protein is highly basic, especially in its C-terminal region (Figure 12), suggesting that this region could be important for Dsup protein to associate with DNA. As the C-terminal

region of Dsup protein was sufficient for localization of Dsup protein to around nuclear DNA (Figure 13a, c), I examined whether the C-terminal region was responsible for the DNA-associating activity. The C-terminal region alone was sufficient to shift the DNA mobility in a manner similar to that of full-length Dsup protein (Figure 14). In contrast, Dsup protein lacking the entire C-terminal region (Dsup Δ C) completely lost the ability to shift the DNA mobility (Figure 14). These findings indicated that the C-terminal region of Dsup is necessary and sufficient for the ability of Dsup protein to associate with DNA as well as to localize around nuclear DNA.

Requirement of the C-terminal region of Dsup protein for DNA protection activity in Dsup-expressing cells.

As the C-terminal region was necessary and sufficient for both localization around nuclear DNA and DNA associating ability of Dsup protein, I postulated that the C-terminal region alone could be sufficient to suppress DNA damage. To test this possibility, I tried several times to generate stable cell lines expressing Dsup-C. However, I was unable to obtain any strain that proliferated normally and stably expressed Dsup-C. As shown in Figure 13b and Figure 13c, Dsup-C affected the distribution of nuclear DNA and thus it is possible that Dsup-C interferes with DNA replication and/or transcription, thereby preventing cell proliferation. On the other hand, I was able to establish a stable line expressing Dsup Δ C, which lacks the C-terminal DNA-associating region and localizes mainly in the cytoplasm (Figure 15).

I next examined whether Dsup Δ C cells exhibit improved DNA protection from X-ray irradiation using an alkaline comet assay. The Dsup Δ C-expressing cells exhibited no reduction in the proportion of fragmented DNA in the alkaline comet assays when compared to untransfected HEK293 cells (Figure 16a, Table 1 and 2), suggesting that the ability to

associate with DNA is a prerequisite for Dsup to protect DNA from X-ray irradiation. In addition, the reduction of the number of γ -H2AX foci by Dsup was partially impaired in the Dsup Δ C-expressing cells (Figure 16b, Table 7 and 9), consistent with the importance of DNA-associating ability in the DNA protection activity of Dsup protein. Furthermore, I examined whether the cells expressing a Dsup mutant lacking the DNA-associating domain (Dsup Δ C) also exhibit the improved radio-tolerance. The improvement in radio-tolerance was impaired in Dsup Δ C-expressing cells compared to those in full-length Dsup expressing cells (Figure 17 and Table 10), suggesting that DNA-targeting is also important for full improvement of the radio-tolerance by Dsup.

Discussion

In Chapter 2, I defined three distinct regions in Dsup protein based on *in silico* analysis and assessed the functional properties of each region. To identify the region responsible for nuclear translocation, I created various mutants lacking the N-terminal region, α -helical region or C-terminal regions of Dsup protein, examined their subcellular localization and found that the C-terminal region was necessary and sufficient for nuclear localization (Figure 13a). I also showed that the C-terminal region of Dsup is essential for association with DNA *in vitro* (Figure 14), suggesting that association with DNA is important for the nuclear localization of Dsup protein to DNA. The stably Dsup Δ C-expressing cells exhibited no reduction in the proportion of fragmented DNA compared to HEK293 cells (Figure 16a). Furthermore, suppression of DNA double-strand breaks was partially impaired in the Dsup Δ C-expressing cells (Figure 16b), suggesting the importance of DNA-associating ability in the DNA protection activity of Dsup protein. Dsup Δ C-expressing cells also exhibited impaired an improvement of radio-tolerance compared to full-length Dsup-expressing cells (Figure 17). These results suggest that DNA-association activity is important for the full improvement of the radio-tolerance by Dsup.

To my knowledge, this is the first report to demonstrate that a DNA-associating protein derived from an extremotolerant animal improves DNA-protection and tolerance for X-ray irradiation in human cultured cells. In some bacteria, including *Escherichia coli*, a ferritin-like DNA-associating protein termed Dps forms giant complexes with DNA in non-proliferative conditions and physically protects DNA from oxidative stress [Almiron, M. *et al.* (1992); Frenkiel-Krispin D. *et al.* (2001)]. As shown in Figure 14, both the full-length Dsup and Dsup-C proteins drastically shifted the mobility of DNA in gel shift assay (Figure

14). The absence of band with intermediate mobility shift suggested that Dsup protein forms a huge complex with DNA. Such huge complex formation might be beneficial to physically shield DNA from environmental stresses, as *E. coli* Dps does. On the other hand, it likely interferes with DNA replication and transcription. Overexpression of several DNA-associating proteins, such as a bacterial histone-like nucleoid-structuring (H-NS) protein or a small acid-soluble spore protein (SASP) associated with spore DNA of *Bacillus subtilis*, causes severe condensation of DNA and loss of cell viability [Setlow, B. *et al.* (1991); Spurio R. *et al.* (1992)]. In the case of *E. coli* Dps, formation of Dps protein-DNA complex appears only in the stationary condition and low demands on DNA transaction might relieve adverse effects by heavy binding of Dps proteins to DNA. In contrast, as shown in Figure 17, Dsup-expressing human cultured cells proliferated faster than untransfected cells and simultaneously acquired DNA-protection ability. To avoid negative effects of huge protein-DNA complex formation on transcription and DNA replication, there may be a regulatory mechanism of complex formation.

Expression of truncated Dsup containing the C-terminal DNA-associating region alone induced an abnormal aggregation of nuclear DNA (Figure 13b,c), possibly due to sporadic hyper-compaction or heavy heterochromatinization and I was unable to establish stable cell lines expressing the C-terminal region only. Presumably, the association of Dsup-C with DNA is not favorable and may be even toxic for transfected cells. In contrast, full-length Dsup-expressing cells exhibited an almost normal distribution of nuclear DNA, similar to that in control HEK293 cells (Figure 18). Further, full-length Dsup-expressing cells proliferated rather faster than untransfected cells (Figure 17), suggesting that the presence of the N-terminal and middle regions are important to relieve the adverse effects (e.g., possible heterochromatinization and/or interference on transcription and replication) induced by the association of proteins with DNA. It is possible that this feature of Dsup protein enables

DNA protection without impairing cell viability, which could be suitable for future application of Dsup to confer a tolerance to the other animal cells.

Conclusion and Future Perspectives

In this thesis, I used human cultured cells to investigate function of a novel DNA-associating protein, termed Damage suppressor (Dsup), that was isolated from a chromatin fraction of *R. varieornatus* as a candidate protein involved in radiation tolerance. Stable expression of Dsup protein in human cultured cells significantly suppressed DNA breaks caused by X-ray irradiation and hydrogen peroxide. Furthermore, after 4 Gy X-ray irradiation, some fraction of Dsup-expressing cells survived and even retained proliferative ability.

Based on these findings, I conclude that Dsup protein improves radio-tolerance of human cultured cells (Figure 19). Dsup protein is, to my knowledge, the first DNA-associating protein, identified from an extremotolerant animal, to be demonstrated to protect DNA and improve the radio-tolerance of cultured animal cells. Association of Dsup protein with nuclear DNA could be beneficial to suppress X-ray induced DNA damage through physical shielding or protection from indirect radiation effects (reactive oxygen species, ROS). The precise relationship between DNA protection and improvement in radio-tolerance, however, remains elusive at present. To reveal the relationship between them, (1) determination of precise mode of interaction between Dsup and nuclear DNA, (2) analysis of whether Dsup can protect DNA only from indirect effects caused by ROS or even from direct effects using α -particle irradiation, and (3) investigation into whether the improved radio-tolerance of Dsup protein can also be observed in different cell type or in tardigrade would be helpful.

As for the above 1st subject, Dsup protein has ability to associate with DNA, but the mode of interaction between Dsup and nuclear DNA is unclear. To examine the precise mode of the interaction, it might be effective to perform gel shift assays using nucleosome or

chromatin instead of naked DNA *in vitro*. The observation of the complexes composed of chromatin (or nucleosome) and Dsup protein using atomic force microscope might be beneficial to analyze the mode of interaction. These assays are expected to provide more insights into the association of Dsup protein with nuclear DNA.

As for the above 2nd subject, I showed in Chapter 1 that Dsup protein protected DNA from oxidative stress, suggesting that DNA protection by Dsup protein from X-ray irradiation is at least partially through counteraction against ROS indirectly generated by X-ray irradiation. To examine whether Dsup can also counteract against direct effects, I plan an irradiation experiment of α -particle to Dsup-expressing cells. I expect that this experiment could provide more direct solution of this subject, because α -particle irradiation causes mostly only direct effects. Direct effects of irradiation are truly physical phenomena and are unlikely to be interfered by protein molecules such as Dsup. Thus, at this moment, I suppose that DNA damage would similarly occur in both Dsup-expressing cells and untransfected cells upon α -particle irradiation. If similar DNA fragmentation is detected in both Dsup-expressing cells and untransfected cells in comet assays after α -particle irradiation, it may also argue against the possibility that Dsup protein could tolerate alkaline condition and thus interfere with the mobility of fragmented DNAs in alkaline comet assays.

As for the above 3rd subject, I used HEK293 cells to investigate the improvement of radio-tolerance. HEK293 cells are a kind of immortalized human cultured cell lines, which are potentially pre-adapted to stressful and oxidative environments in the artificial culture system. Therefore, it could be possible that Dsup protein might have enhanced radio-tolerance in conjunction with the partially pre-adapted characteristics of the cultured cells. To reveal that Dsup protein alone is sufficient to confer DNA protection activity, it may be necessary to test the effect of Dsup protein using normal cells, e.g., human fibroblasts. Such trials may be important to widen the application of Dsup protein as radio-protective

reagents to more general purposes, including clinical applications.

Although DNA protection and improvements of radio-tolerance were examined only in human cultured cells, Dsup proteins exhibited similar localization around nuclear DNA in all examined cells, i.e., human cultured cells, insect S2 cells and tardigrade cells. Supposing that the association of Dsup protein with nuclear DNA is regulated in a similar manner beyond animal species, it seems possible that Dsup could also confer DNA protection activity to non-human eukaryotic organisms. Then, is Dsup protein also involved in the extraordinary radio-tolerance in the tardigrade itself? To answer this question, it is necessary to perform a loss-of-function analysis by targeting *Dsup*. Till now, RNA interference has successfully been adapted to tardigrades [Tenlen, J. R. *et al.* (2012)], but knockdown experiments are sometimes difficult to draw solid conclusions due to insufficient suppression. Recent advances in genome editing technology have enabled efficient gene knockout experiments in many organisms including non-model animals. Establishment of a genome editing approach, e.g., CRISPR-Cas9, in the tardigrade, could be a next key step, which will provide us powerful tools to elucidate molecular mechanisms underlying the radio-tolerance of tardigrades.

Although Dsup-expressing human cultured cells exhibited improved tolerance to 4 Gy of X-ray irradiation, *R. varieornatus* exhibits extreme tolerance against high-dose irradiation, such as 4,000 Gy of He-ion beam in adults [Horikawa, D. D. *et al.* (2008)], and 500 Gy in active embryos ($LD_{50} \sim 500$ Gy) [Horikawa, D. D. *et al.* (2012)]. Therefore, there may be additional factors besides Dsup protein that contributes to the extreme tolerance in tardigrade. If some of such factors form a complex with Dsup protein, chromatin immunoprecipitation using anti-Dsup antibody would be useful to identify such proteins.

Finally, high dose radiation such as 4,000 Gy is not a common environmental stress on the earth, and could not have been an adaptive pressure for organisms during evolution.

Instead, desiccation is much more common stress and causes severe oxidative stress [França, M. B. *et al.* (2001)] similar to indirect effects of X-ray irradiation. Thus, desiccation-tolerant animals including tardigrades should have the ability to mitigate this type of stress. Indeed, many desiccation-tolerant animals, e.g., tardigrades, bdelloid rotifers and a sleeping chironomid, tolerate high dose irradiation as well as severe dehydration. Based on these suppositions and observations, radiation tolerance of these organisms has been considered to be an evolutionary consequence of the adaptation to desiccation stress [Mattimore, V. *et al.* (1996); Hespeels, B. *et al.* (2014)]. The direct experimental evidence to support this hypothesis, however, has not been presented. The loss-of-function analysis of Dsup protein and co-factors in tardigrade could be the first experimental evidence for the presence of common mechanisms shared by desiccation and radiation tolerances. Unveiling the molecular mechanisms underlying tardigrade extremotolerance will provide novel clues that open new avenues to confer stress resistance to intolerant species, including humans.

Materials and Methods

Animals

The YOKOZUNA-1 strain of the anhydrobiotic tardigrade *R. varieornatus* was used for all experiments. The strain was established from a single individual in previous work [Horikawa, D. D. *et al.* (2008)]. The strain was reared on water-layered agar plates by feeding it alga, *Chlorella vulgaris* (Chlorella industry), at 22°C, essentially as described previously [Horikawa, D. D. *et al.* (2008)].

Subcellular localization analysis of GFP-fusion protein

For expression of GFP-fused full-length Dsup protein, the coding sequence of *Dsup* was amplified and inserted into Asp718 and BamHI sites of pAcGFP1-N1 (Clontech). HEK293T cells were transiently transfected with the construct using X-tremeGENE 9 reagent (Roche) following the manufacturer's protocol. After 24 h, the cells were stained with Hoechst 33342 (Lonza) to visualize nuclear DNA. Fluorescent signals were observed under a confocal microscope (LSM710, Carl Zeiss).

Immunohistochemistry

Anti-Dsup antibody was raised and affinity-purified against bacterially-expressed Dsup protein. Immunohistochemistry on frozen sections of tardigrade embryos was performed essentially as described previously with slight modification [Tanaka, S. *et al.* (2015)]. Tardigrade embryos within 3 days after egg-laying were fixed with 4% paraformaldehyde at room temperature (RT) for 15 min, and were embedded in Agarose-LGT (Nacalai Tesque). The embedded gels were incubated in sucrose series, 15% and 30% overnight each at 4°C and embedded in O.C.T. Compound (Sakura Finetek Japan). Cryosections (10-14 μm

thickness) were prepared using a cryostat (Leica CM1850, Leica). After three washes with 0.1% Tween 20 in Tris-buffered saline, the sections were blocked with 2% goat-serum for 1 h and reacted with the affinity-purified anti-Dsup antibody overnight at 4°C and then with Alexa Fluor 488 anti-Rabbit IgG (Molecular Probes, A-11008) for 45 min at RT. Nuclear DNA was counterstained with 4',6-diamidino-2-phenylindole (DAPI; Invitrogen). Fluorescent signals were observed using a confocal microscope (LSM710, Carl Zeiss).

***In silico* analysis based on the Dsup protein sequence**

Secondary structures were predicted by the CLC main workbench 6.9.1 (CLC Bio). The nuclear localization signal was predicted using the cNLS Mapper (<http://nls-mapper.iab.keio.ac.jp/>). A hydrophobicity plot was generated by ProtScale (<http://web.expasy.org/protscale/>) with the Kyte & Doolittle model [Kyte, J. *et al.* (1982)]. A protein charge plot was generated using EMBOSS [Rice, P. *et al.* (2000)]. Subcellular localizations were predicted by WoLF PSORT [Horton, P. *et al.* (2007)] and TargetP [Emanuelsson, O. *et al.* (2000)].

DNA electrophoretic mobility shift assay

The protein-DNA association was examined by a gel shift assay essentially as described previously [Martinez, A. *et al.* (1997)]. Recombinant Dsup protein was produced as follows. The coding sequence of Dsup was amplified and inserted into NdeI and XbaI sites of pCold-I vector (TaKaRa), which contains the 6xHis tag at the N-terminus. The construct was transformed to BL21 (DE3) cells and protein production was induced with isopropyl β -D-1-thiogalactopyranoside and cold treatment according to the manufacturer's protocol. Recombinant Dsup protein was purified with Ni-NTA His-Bind Superflow (Novagen) in denaturing conditions using 8 M Urea and dialyzed in PBS using a Micro-Dialyzer (Nippon

Genetics). PBS was prepared from 10 times concentrated stock solution (Wako, 163-25265). As a DNA probe, pBluescript II plasmid DNA was linearized by digestion with HindIII and subjected to the assay. Purified recombinant Dsup proteins (10, 50, 75 or 100 ng) were incubated with purified linearized pBluescript DNA (10 ng) in PBS for 20 min at RT. Purified histone H1 protein (bovine) was purchased from Upstate and was used as a positive control. After the incubation, the samples were mixed with gel loading dye (10 mM Tris-HCl pH 8.0, 1 mg/mL bromophenol blue, 20% glycerol) and were electrophoresed in a 0.5% agarose gel in Tris-borate-EDTA (TBE) buffer. DNA was stained with SYBR Green I, and visualized by a transilluminator (ATTO).

Cell lines

HEK293 cells (RCB1637) and HEK293T cells (RCB2202) were obtained from RIKEN BioResource Center (BRC). The identity of these cell lines was validated by STR profiling and all cell lines were negative for mycoplasma contamination (RIKEN BRC). The cells were maintained in Dulbecco's modified essential medium (Nacalai Tesque) containing 10% fetal bovine serum (Corning). A Dsup expression vector was constructed by inserting the coding sequence of Dsup into KpnI and NotI sites of pCXN2KS, a modified pCAGGS vector [Niwa, H. *et al.* (1991)]. The expression construct was transfected to HEK293 cells using X-tremeGENE 9 DNA Transfection Reagent (Roche) and stably transfected cells were selected by 700 µg/ml G418 (Calbiochem) treatment for 3 weeks. I observed many cells with an abnormal morphology (e.g., giant-cells or elongated form) and those cells could not be maintained. Clonal cell populations were obtained by limiting dilution, and Dsup expression was examined by Western blotting analysis and immunohistochemistry. Clones showing non-nuclear localization of Dsup protein immunoreactivity were discarded. The clone expressing the highest level of Dsup protein with nuclear localization was chosen. The target

sequence for the shRNA was designed based on the online analysis software siDirect [Naito, Y. *et al.* (2009)] and BLOCK-iT RNAi Designer (<http://rnaidesigner.lifetechnologies.com/rnaiexpress/>) as 5'-GAA CGT AAC CGT TAC CAA AGG-3'. To construct a vector expressing shRNA, oligonucleotides encoding the stem-loop shRNA sequence were synthesized and inserted into the AgeI-EcoRI site of pLKO.1 puro [Stewart, S. A. *et al.* (2010)]: the inserted sequence was 5'-ACC GGT GAA CGT AAC CGT TAC CAA AGG TTC AAG AGA CCT TTG GTA ACG GTT ACG TTC TTT TTG AAT TC-3'. The shRNA expression construct was transfected to the *Dsup*-expressing stable cell line. After selection by 2 µg/ml puromycin (Sigma) treatment, cell cloning was performed as described above.

Quantification of *Dsup* transcript by real-time RT-PCR

The quantification RT-PCR was performed to estimate *Dsup* expression in *Dsup*-knockdown cells with shRNA. Total RNA was extracted from cell pellet using the RNeasy mini kit following the manufacturer's instructions (Qiagen) and reverse-transcribed using PrimeScript RT reagent Kit with gDNA Eraser (Perfect Real Time; TaKaRa). *Dsup* expression was quantified by real-time PCR using LightCycler 480 Instrument II (Roche) and knockdown efficiency was calculated. Human β -actin was used as an internal control for normalization. Sequences for primer sets were as follows:

Dsup: Forward 5'-TCC ACA GAA CCC TCT TCC AC-3'; Reverse 5'-TCT TGA CAA TGG CAG CTG AG-3'. β -actin: Forward 5'-TGA GCG CGG CTA CAG CT-3'; Reverse 5'-TCC TTA ATG TCA CGC ACG ATT T-3'.

Comet assay

A comet assay was performed using the CometAssay Kit (Trevigen) under alkaline or neutral

conditions essentially according to the manufacturer's protocol. Briefly, cells were irradiated on ice using an X-ray generator, the Pantak HF 350 (Shimadzu) operating at 200 kV–20 mA with a filter of 0.5 mm Cu and 1 mm Al at a fixed dose rate of 1.73 Gy/min. I selected irradiation doses that increased the proportion of tail DNA to a 30% to 50% of total DNA to clearly visualize the irradiation-dependent increase of DNA damage without catastrophic fragmentation (10 Gy and 5 Gy were used for alkaline or neutral conditions, respectively). The irradiated cells were immediately trypsinized and collected as a cell suspension. Cell suspensions were mixed with molten agarose and solidified as a thin layer on slide glasses by chilling at 4°C for 30 min. For alkaline comet assays, the slide glasses were soaked for 1 h in manufacturer's lysis solution (3.72% ethylenediaminetetraacetic acid (EDTA), 1% SDS, 1% Triton X-100, Trevigen) at 4°C for 1 h to lyse the cells, and then immersed in alkaline solution (200 mM NaOH, 1 mM EDTA, pH > 13) for 1 h at room temperature, in the dark and electrophoresed in freshly prepared alkaline solution at 25 V and 4°C for 1 h. For neutral comet assay, the cells-mounted slide glasses were soaked in the lysis solution (2.5 M NaCl, 10 mM Tris, 100 mM EDTA, 1% sarcosinate, and 0.01% Triton X-100) at 4°C [Kitta, K. *et al.* (2001)], and then washed in TBE buffer for 30 min and electrophoresed in freshly prepared TBE buffer at 25 V and 4°C for 1 h. After electrophoresis, the comets were visualized by staining with SYBR Green I and captured with an Imager Z1 (Carl Zeiss). DNA fragmentation was quantified for at least 120 comets per condition using CASP software [Końca, K. *et al.* (2003)].

Hydrogen peroxide (H₂O₂) treatment

Cells were treated with 100 µM hydrogen peroxide (H₂O₂) at 4°C for 30 min. Half of the cells were pretreated with an antioxidant, 10 mM N-acetyl-L-Cysteine (NAC, Sigma) for 30 min prior to the hydrogen peroxide treatment. DNA damage was evaluated by the alkaline

comet assay with the electrophoresis at 25 V at 4°C for 30 min, immediately after the treatment. At least 302 comets were analyzed for each condition.

γ -H2AX foci detection

The cultured cells on Chambered Coverglass (Thermo Scientific) were irradiated with 1 Gy of X-ray using the Pantak HF 350 X-ray generator (Shimadzu). One hour after X-ray irradiation, the cultured cells were fixed with 4% formaldehyde for 15 min and permeabilized with 0.5% Triton X-100 for 15 min. The cells were blocked with 10% goat-serum for 1 h and reacted with the anti-phospho-histone H2A.X (Ser139) antibody clone JBW301 (Merck Millipore, 05-636) for 1 h and then with Alexa Fluor 488 anti-mouse IgG (Molecular Probes, A-11001) for 45 min. Nuclear DNA was counterstained with DAPI (Invitrogen). All reactions and procedures were essentially performed at RT. Fluorescent signals were observed by confocal microscopy (LSM710, Carl Zeiss). The depth-coded projections were captured as stacks of 10 optical sections of z-series at 1- μ m intervals, and converted to binarized images by ImageJ version 1.47. To avoid overlap of multiple foci and minimize corresponding counting errors, the threshold value for automated counting was manually adjusted until a visual best fit between the original and converted images was observed (Figure. 20). The numbers of γ -H2AX foci were counted as previously described [Cai, Z. *et al.* (2009)].

Cell cycle analysis

Cell cycle analysis was essentially performed as described previously [Nassour, J. *et al.* (2016)]. 5-Bromo-2-deoxyuridine (BrdU, Sigma) was added to cell cultures at 10 μ M at 37 °C for 1 h. The pulse-labeled BrdU cells were collected as a cell suspension after trypsinisation. Cells were fixed with 90% ice-cold ethanol and gentle vortexing, and

incubated on ice for 1 h. Cells were rinsed in PBS and further incubated with 2 N HCl / 0.5% Triton X-100 at RT for 30 min. After that, cells were suspended in 0.1 M sodium tetraborate for 30 min. Cells were incubated with anti-BrdU mouse IgG (555627, BD Pharmingen) at RT for 1 h and incubated with Alexa Fluor 488 Goat anti-mouse IgG (Molecular Probes, A-11001) for 30 min after two washes with PBS. Cells were finally incubated with PBS containing 10 µg/ml RNase (Sigma) and 5 µg/ml propidium iodide (Dojindo) at RT for 30 min in the dark and then filtered through 77-µm nylon mesh to remove cell clusters. Cells were analyzed by flow cytometry using BD FACSVerse (BD Bioscience). At least 10,000 events were collected and data were analyzed using FlowJo software (Tree Star Inc.).

Cell count and measurement of cell viability

Cells were seeded in poly-L-lysine-coated 24-well plates (Iwaki) at a density of 1,000 cells per well. After 24-h incubation (1 day post seeding, dps), the cells were irradiated with 4 Gy of X-ray using the Pantak HF 350 X-ray generator. With 24-h intervals, the cells were incubated with PrestoBlue Cell Viability Reagent (Invitrogen) for 2 h and the fluorescence was measured using a microplate fluorometer, the Spectra max Gemini EM (Molecular Devices) according to the manufacturer's protocol. To count the cell number, the cells were washed gently with PBS and treated with trypsin, then recovered as a cell suspension at 8, 10, and 12 dps. The numbers of cells in the suspensions were counted using an automatic cell counter, the Z1 Particle Counter (Beckman Coulter). I examined three wells for each condition.

Statistical analysis

The effects of Dsup or its derivatives in alkaline/neutral comet assays, γ-H2AX assays, and cell viability assays were evaluated by statistical tests. For pairwise comparisons, Student's

t-test or Welch's *t*-test was used depending on the equality of variance between samples determined by F-test (significance level = 0.05). For comparisons among three samples, Tukey-Kramer's test was used to evaluate the differences between all possible comparison pairs. All statistical measures and tests of the comet assays, γ -H2AX assays, and cell viability assays are provided in Tables 1-10.

Figures

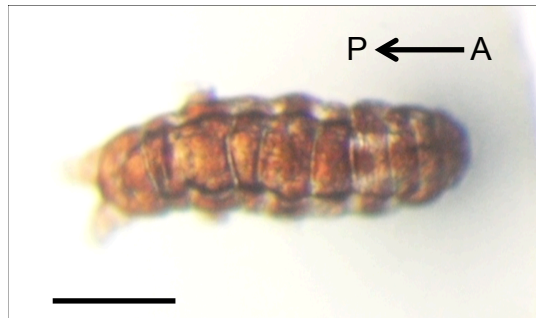


Figure 1. The extremotolerant tardigrade, *Ramazzottius varieornatus*

The stereo-microscopy image of the extremotolerant tardigrade, *R. varieornatus*. Scale bar, 100 μm . A; anterior. P; posterior.

Dsup **MASTHQSSSTEPSSSTGKSEETKKDASQGSQGD SKNVTVTKGTGSSATSA**

Dsup **AIVKTGGSQGKDSSTTAGSSSTQGQKFSTTPTDPKTFSSDQKEKSKSP**

Dsup **AKEVPSSGDSKSQGDTSQSDAKSSGQSQGQSKDSGKSSSDSSKSHSV**

Dsup **IGAVKDVVAGAKDVAGKAVEDAPSIMHTAVDAVKNAATTVKDVASSAA**

Dsup **STVAEKVVDAVH SVVGDKTDDKKEGEHSGDKKDDSKAGSGSGQGGDNK**

Dsup **KSEGETSGQAESSSGNEGAAPAKGRGRGRPPAAAKGVAKGAAGAAAS**

Dsup **KGAKSGAESSKGGSEQSSGD IEMADASSKGGSDQRDSAATVGEGGASGS**

Dsup **EGGAKKGRGRGAGKKADAGDTSAEPPRRSSRLTSSGTGAGSAPAAAKG**

Dsup **GAKRAASSSSTPSNAKKQATGGAGKAAATKATAAKSAASKAPQNGAGA**

Dsup **KKKGGKAGGRKRK**

Figure 2. The amino acid sequence of Dsup protein

The nucleotide sequence for Dsup coding sequence region was deposited to DDBJ database under the accession number, LC050827. The deduced amino acid sequence is presented.

Dsup protein is composed of 445 amino acids.

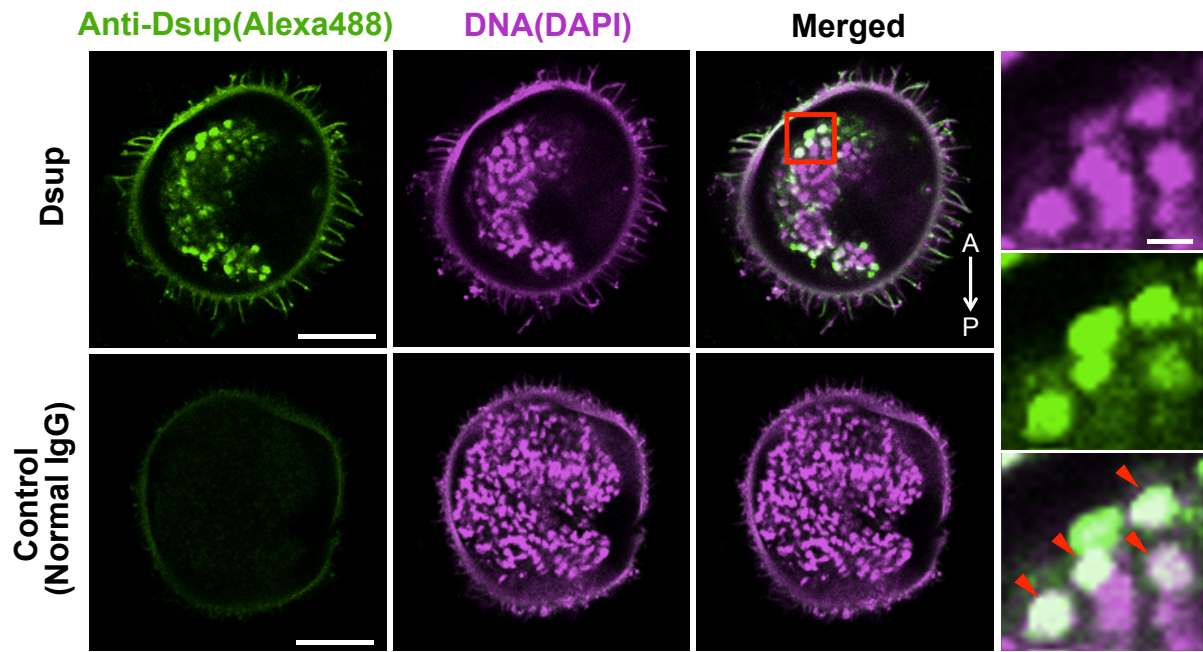


Figure 3. Localization of Dsup proteins around nuclear DNA in embryonic cells of *R. varieornatus*

Immunohistochemical detection of Dsup proteins in a frozen section of tardigrade embryos. DNA stained with DAPI is shown in magenta. Enlarged images corresponding to the red box in the merged picture are shown on the right side. Red arrowheads indicate localization of Dsup proteins around nuclear DNA. A; anterior, P; posterior. Scale bar, 10 μm (In enlarged image, scale bar indicates 2 μm).

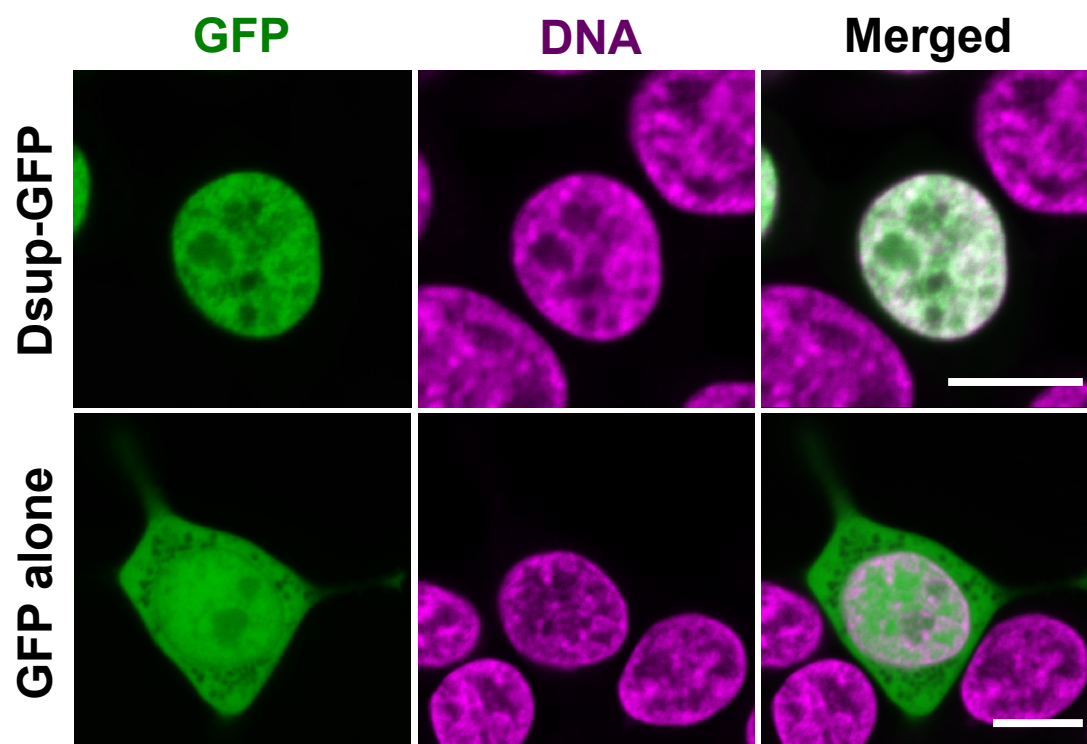


Figure 4. Dsup protein localized around nuclear DNA in human cultured cells

Subcellular localization of Dsup-GFP fusion proteins transiently expressed in HEK293T cells.

Nuclear DNA was visualized by Hoechst 33342. Scale bars, 10 μm .

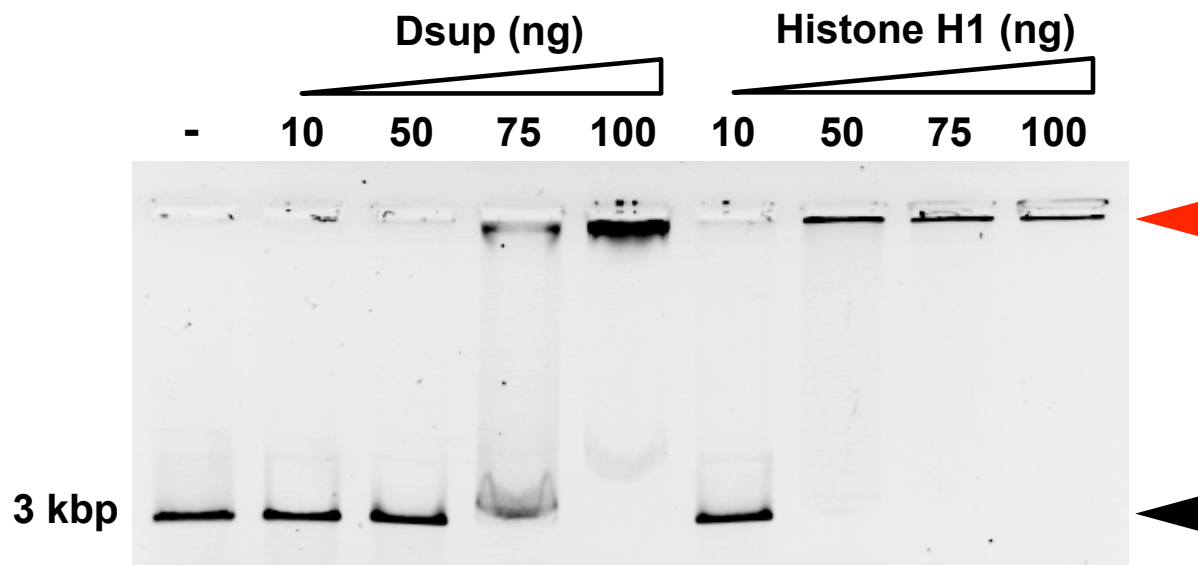


Figure 5. The mobility shift assay of Dsup

Mobility shift of DNA by recombinant Dsup protein in a dose-dependent manner (10, 50, 75 or 100 ng). Black arrowhead indicates the predicted size of the probe DNA (3 kbp, 10 ng). Red arrowhead indicates the position of the extremely slowly migrating DNA in the presence of Dsup protein. A similar extensive mobility shift was observed with histone H1.

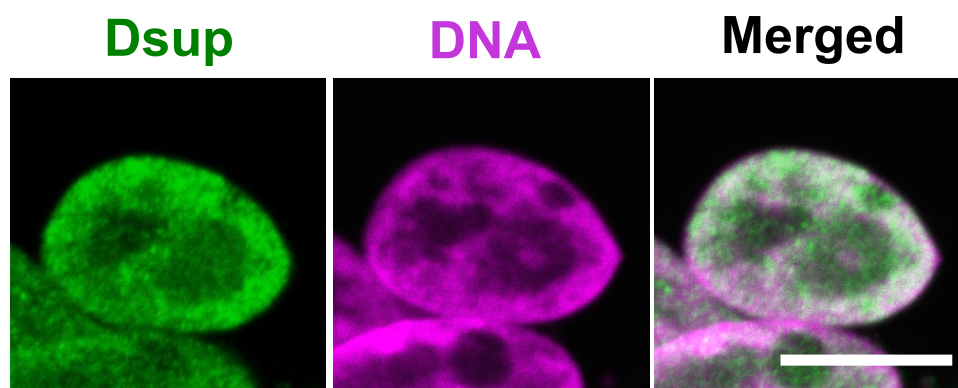


Figure 6. Subcellular localization of Dsup proteins in stably transfected HEK293 cells

Subcellular localization of full-length Dsup proteins was examined by immunocytochemistry in stably transfected HEK293 cells expressing. Nuclear DNA was visualized by DAPI staining. Full length Dsup protein localized around nuclear DNA. Scale bars, 10 μm .

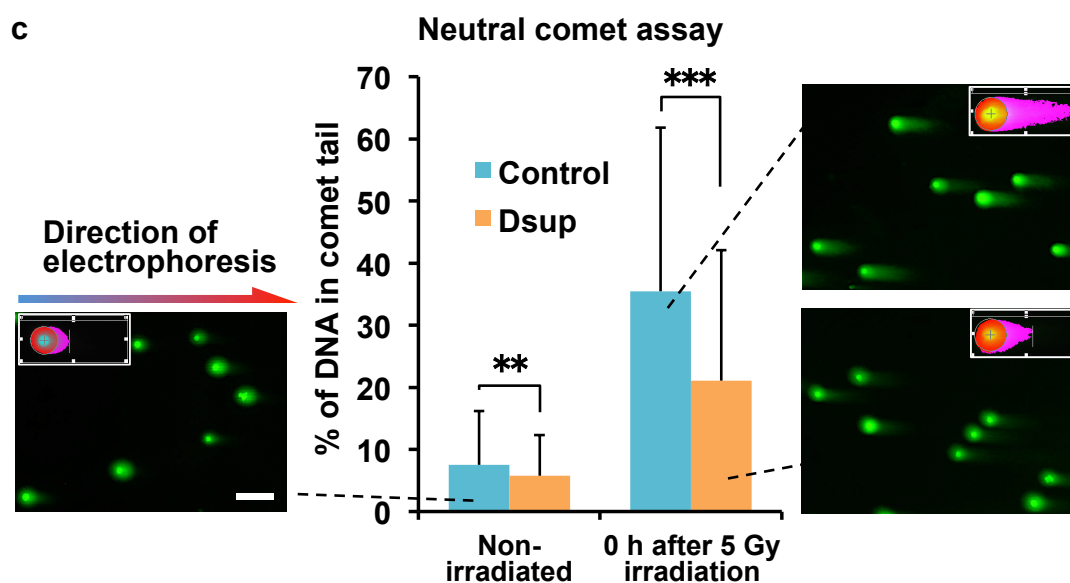
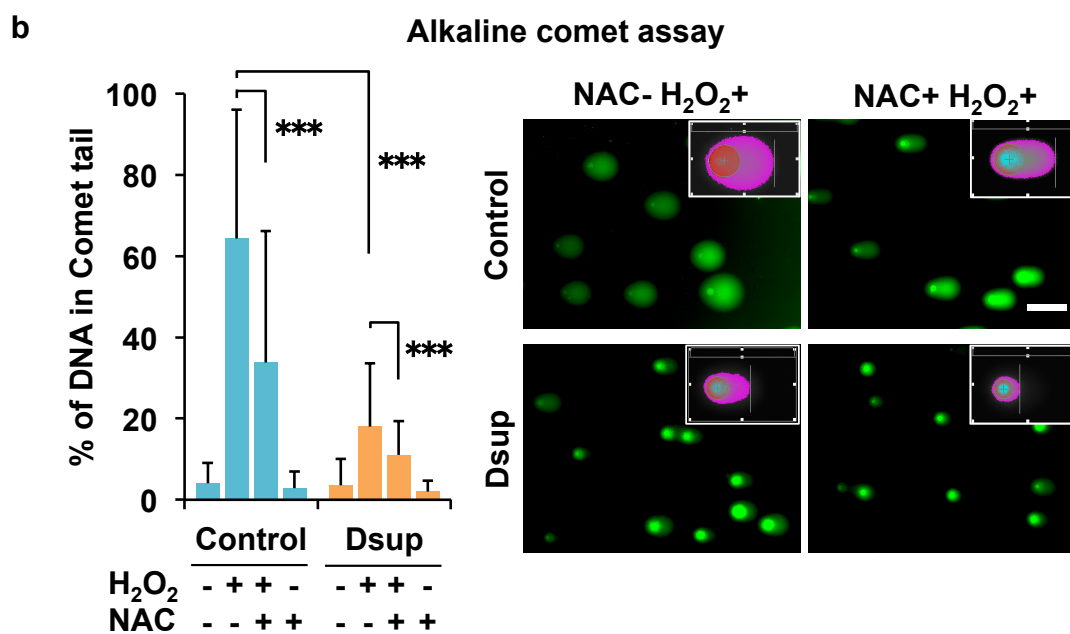
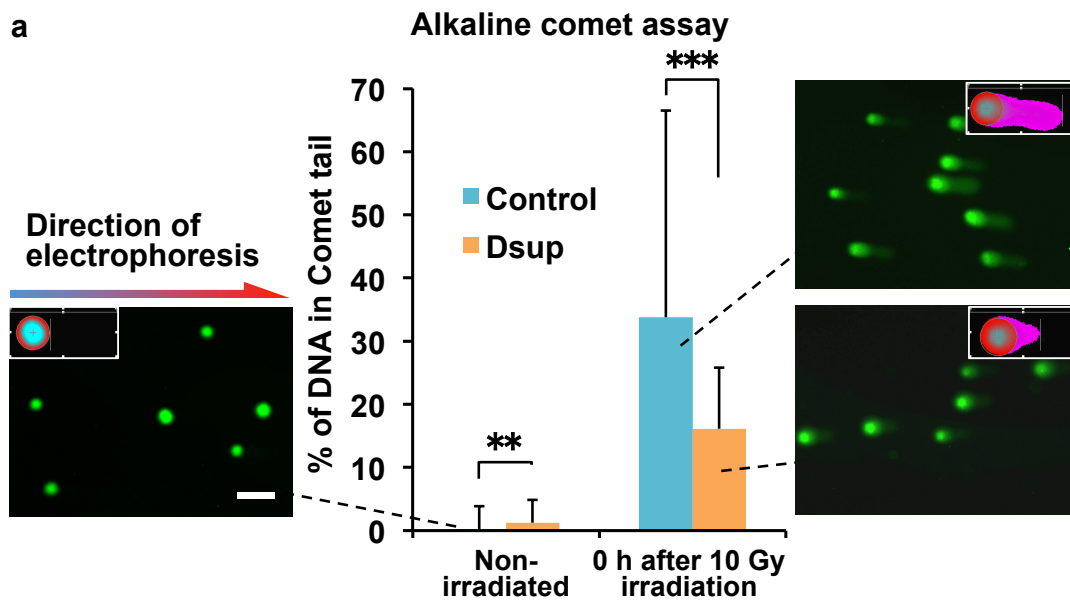


Figure 7. Dsup protein suppresses stress-induced DNA fragmentation in human cultured cells

(a) The effects of Dsup on SSBs by 10 Gy X-ray irradiation in alkaline comet assays. The irradiated cells were immediately subjected to the assay. Representative images are shown for each condition. In the pseudo-colored images in the inset, red to blue circles indicate nuclear DNA and magenta indicates fragmented DNA in tail. DNA fragmentation was assessed by the proportion of DNA detected in the tail region (% of DNA in Comet tail). At least 281 comets were analyzed for each condition. Values represent mean \pm s.d. in all panels. $**P<0.01$, $***P<0.001$ (Welch's *t*-test. Non-irradiated; *t*-value = -3.199, *p*-value = 0.0015. Irradiated; *t*-value = 8.599, *p*-value < 1.0E-15). (b) The effects of Dsup on SSBs caused by hydrogen peroxide (H₂O₂) treatment in alkaline comet assays. Cells were treated with 100 μ M H₂O₂ for 30 min at 4°C to induce DNA damage with or without pretreatment with 10 mM N-acetyl-L-Cysteine (NAC) as an antioxidant for 30 min. At least 203 comets were analyzed for each condition. $***P<0.001$, n.s. indicates not significant (Tukey-Kramer's test). (c) The effects of Dsup on DSBs by 5 Gy X-ray irradiation in neutral comet assays. 300 comets were analyzed for each condition. $**P<0.01$, $***P<0.001$ (Welch's *t*-test. Non-irradiated; *t*-value = 2.758, *p*-value = 0.0060. Irradiated; *t*-value = 7.406, *p*-value = 4.7E-13). Scale bars, 100 μ m.

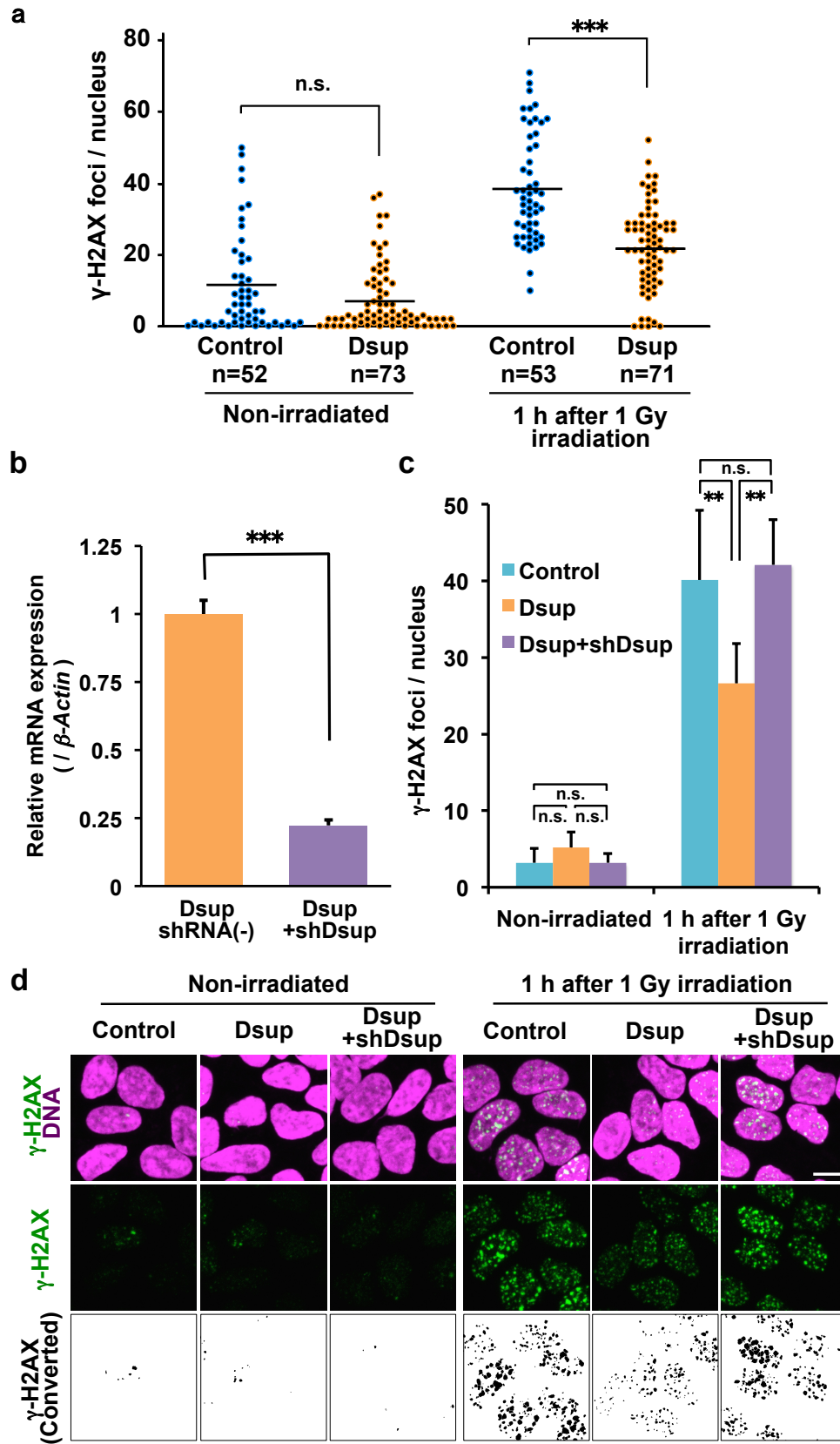


Figure 8. Reduced formation of γ -H2AX foci in human cultured cells depending on Dsup expression

(a) Distribution of the numbers of γ -H2AX foci per nucleus is shown. Each dot represents an individual nucleus of a HEK293 cell (Control) or a Dsup-expressing cell (Dsup) under non-irradiated and irradiated conditions. *** $P < 0.001$, n.s. indicates not significant (Welch's *t*-test). (b) Significant decrease of *Dsup* transcript in shRNA-introduced cells (Dsup+shDsup) compared to that in untreated Dsup-expressing cells (Dsup shRNA(-)). $n=3$. Values represent mean \pm s.e.m. *** $P < 0.001$ (Student's *t*-test). (c) Quantitative comparison of γ -H2AX foci number among untransfected HEK293 cells (Control), Dsup-expressing cells (Dsup), and *Dsup*-knockdown cells (Dsup+shDsup) under non-irradiated and 1 Gy X-ray irradiated conditions. At least 70 cells were analyzed for each condition. Values represent mean \pm s.d.. ** $P < 0.01$, n.s. indicates not significant (Tukey-Kramer's test). (d) Representative images detecting γ -H2AX foci in each condition. Fluorescent images were converted to binary images for automatic counting of foci. Scale bar, 10 μ m.

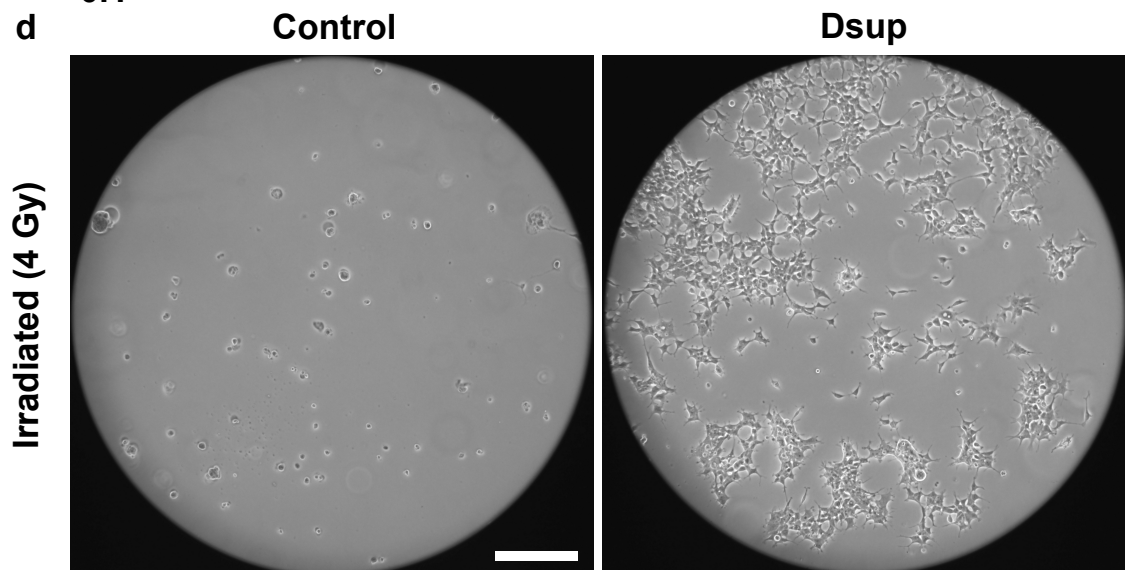
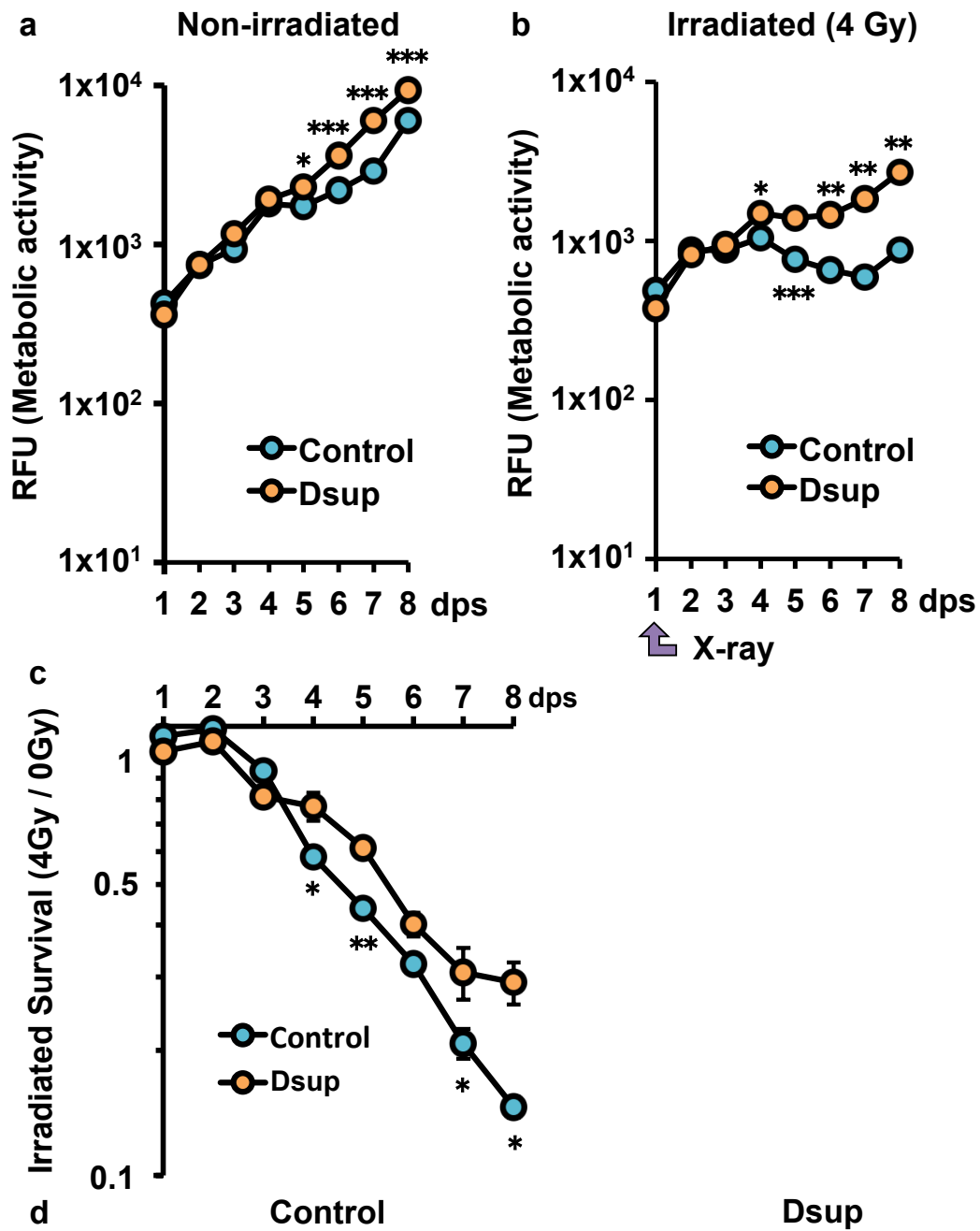


Figure 9. Effect of Dsup on cell viability of human cultured cells under irradiated and non-irradiated conditions

(**a, b**) Comparison of temporal changes in cell viability between untransfected HEK293 cells (Control) and Dsup-expressing cells (Dsup) under non-irradiated (**a**) and irradiated conditions with 4 Gy of X-ray (**b**). Cellular viability was measured using PrestoBlue reagent detecting reducing power of total cells and is shown as mean \pm s.e.m. * $P < 0.05$, ** $P < 0.01$, *** $P < 0.001$, n.s. indicates not significant (Student's *t*-test). RFU, relative fluorescence units. (**c**) Temporal change of irradiated survival, which is cell viability in irradiated condition normalized with that in the non-irradiated condition at the same time point. (**d**) Phase contrast microscopy images of 4 Gy X-ray irradiated cells at 12 dps. dps, days post seeding. Scale bar, 200 μ m.

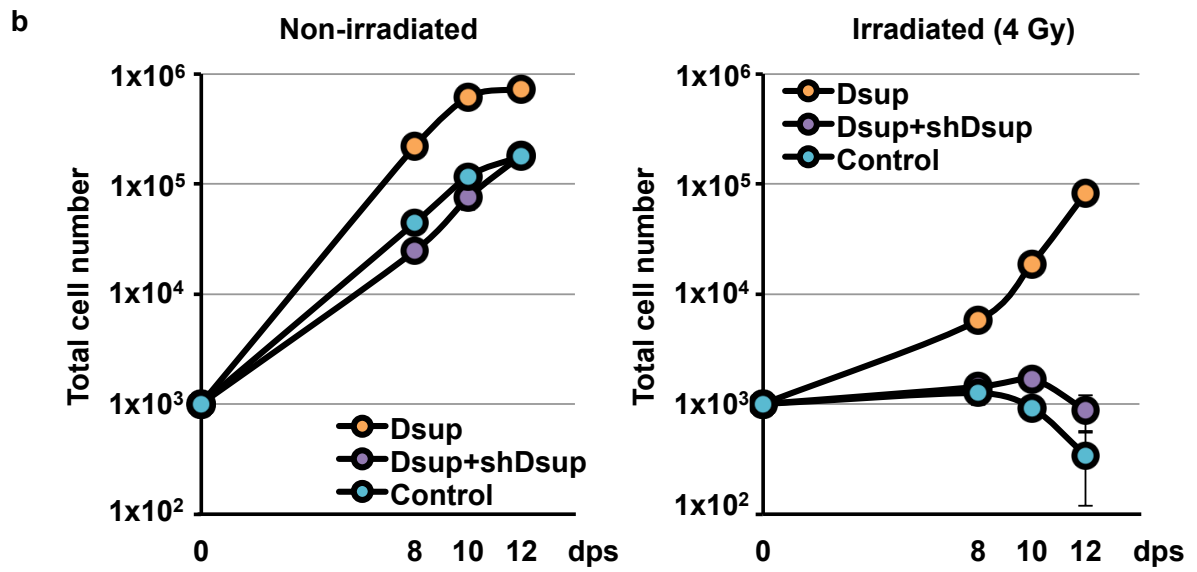
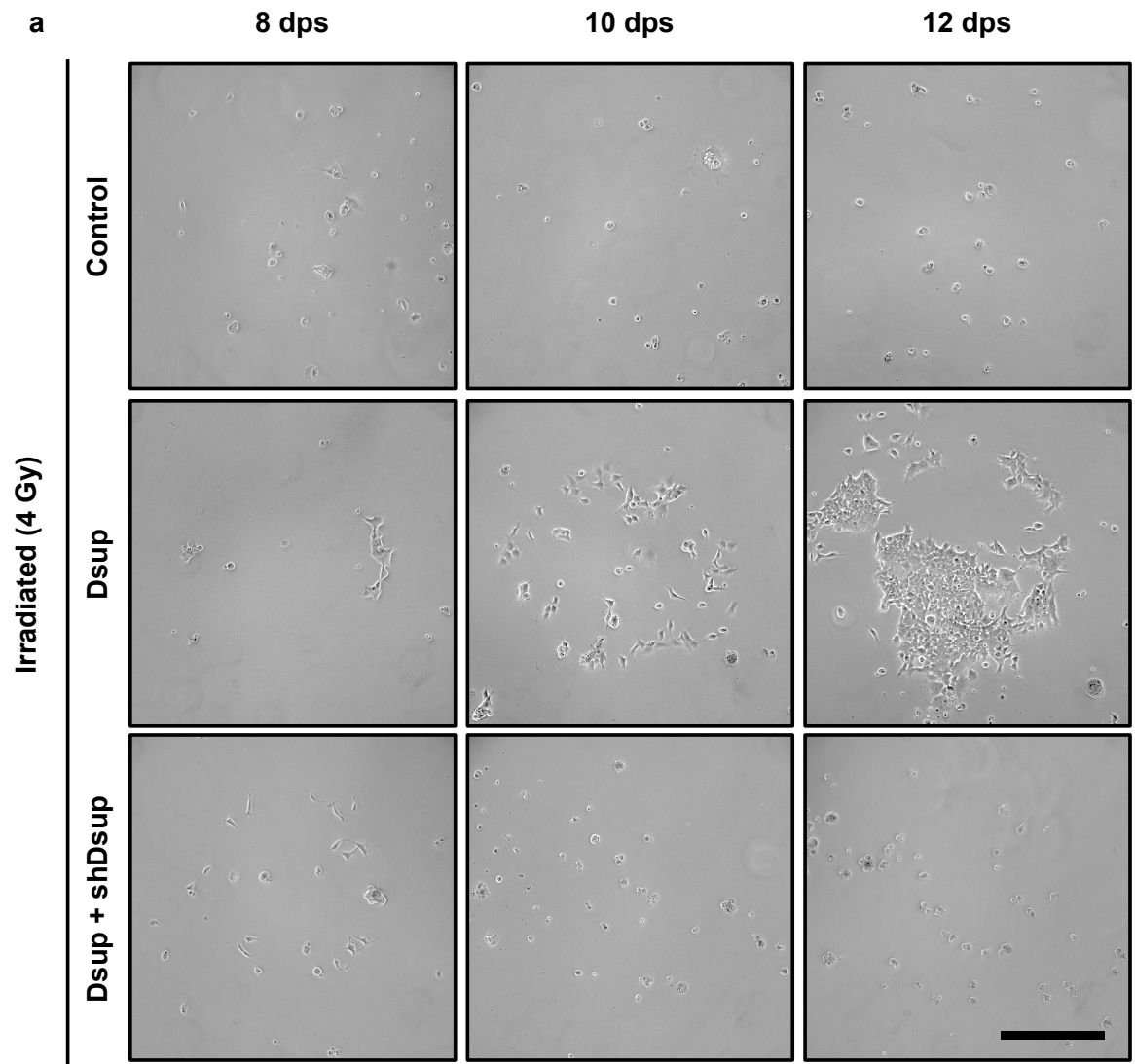


Figure 10. Improved viability and proliferative ability of Dsup-expressing cells after irradiation

(a) Representative microscopic images with phase contrast at 8, 10, and 12 dps, of untransfected HEK293 cells (Control), Dsup-expressing cells (Dsup), and *Dsup*-knockdown cells (Dsup+shDsup) irradiated with 4 Gy X-ray at 1 day post seeding (dps). Scale bar, 200 μ m. (b) Comparison of growth curves of untransfected cells (Control), Dsup-expressing cells (Dsup), and *Dsup*-knockdown cells (Dsup+shDsup) in non-irradiated and irradiated conditions. Values represent mean \pm s.d.

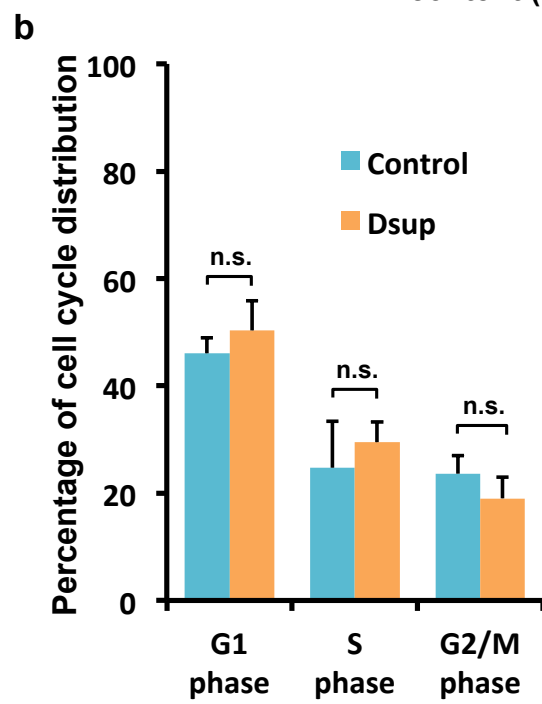
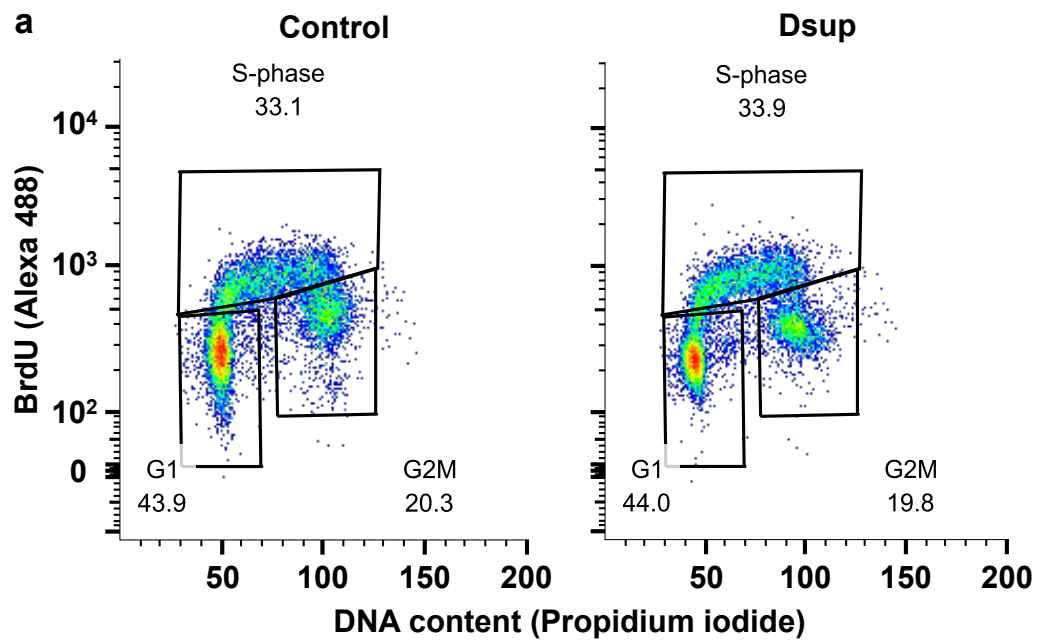


Figure 11. Cell cycle distribution of Dsup-expressing cells

(a) Representative dot plots of cell cycle distribution of HEK293 cells (Control) and Dsup-expressing cells (Dsup). Cell cycle was analyzed by combined propidium iodide and BrdU staining. At least 10,000 events were collected and the distribution of cell cycle phases (G1 phase, S phase and G2/M phase) was calculated using gated regions. (b) Quantitative comparison of cell cycle between HEK293 cells (Control) and Dsup-expressing cells (Dsup) for each phase. The statistical analysis of the three experiments is shown. Values represent mean \pm s.d.. n.s. indicates not significant (Welch's *t*-test. G1 phase; *t*-value = -1.190, *p*-value = 0.320. S phase; *t*-value = -0.872, *p*-value = 0.448. G2/M phase; *t*-value = 1.548, *p*-value = 0.197).

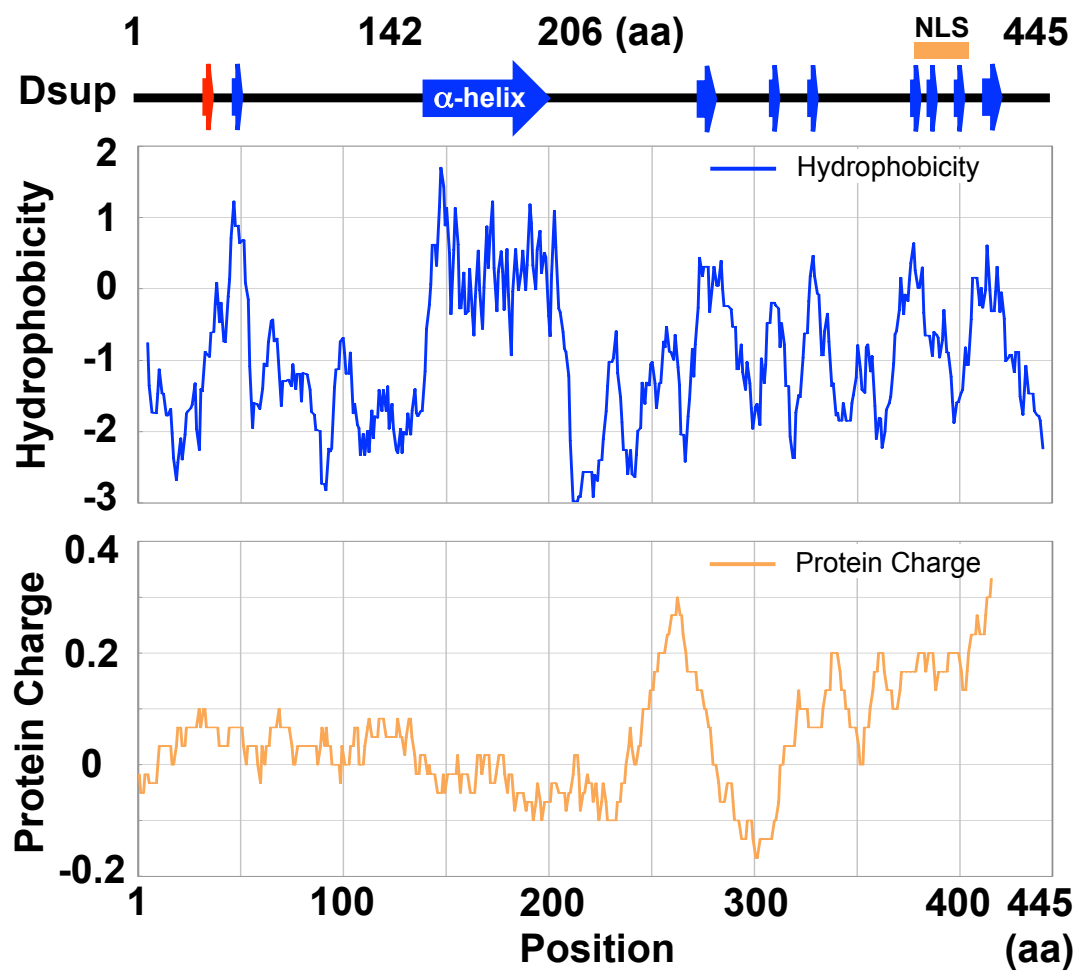


Figure 12. *In silico* analysis based on the Dsup protein primary structure

Schematic representation of Dsup protein with predicted secondary structures and plots of hydrophobicity and protein charges. Blue and red arrows indicate predicted α -helix and β -strand regions, respectively. A putative long alpha-helical region in the middle of the protein (142-206 amino acids, aa) corresponds to a characteristically hydrophobic region in the hydropathy plot. Orange bar around the C-terminus indicates the predicted nuclear localization signal (NLS, 383-404 aa). A charge plot revealed that basic amino acids were enriched in the C-terminal region, suggesting potential involvement of the C-terminal region in the nuclear localization and DNA-association.

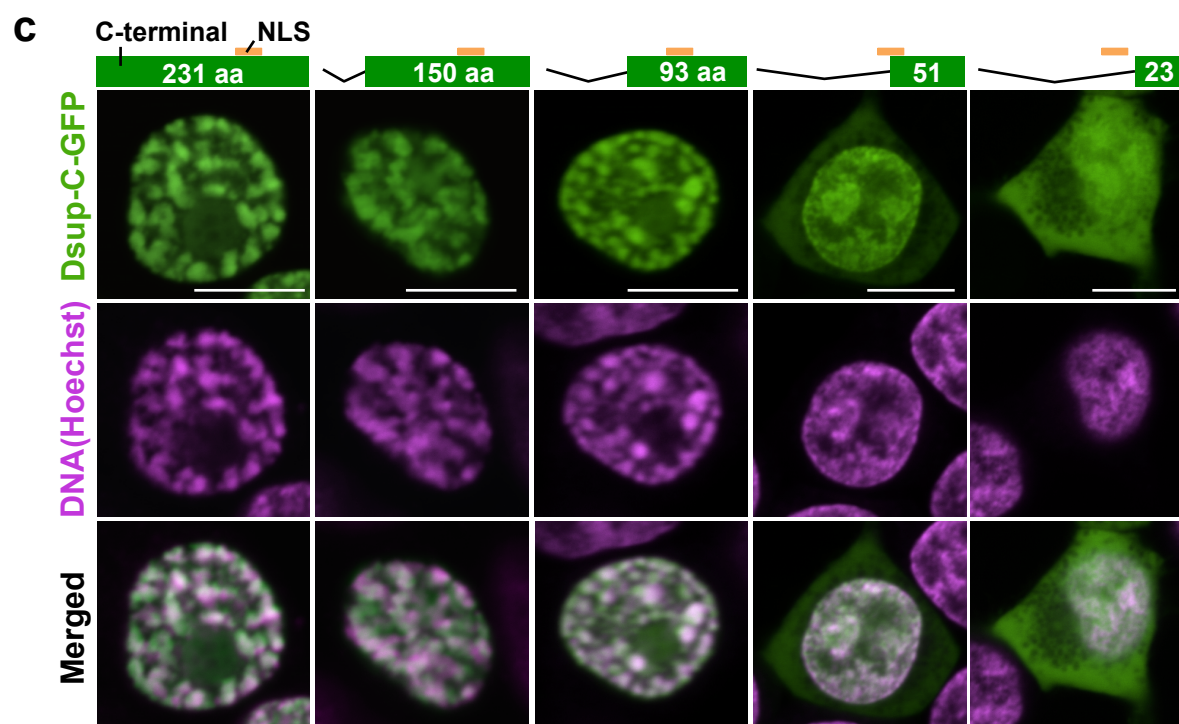
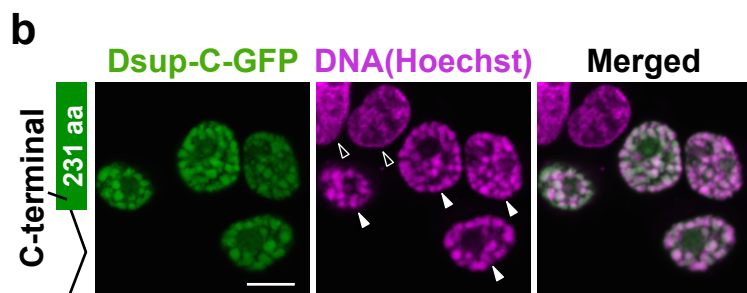
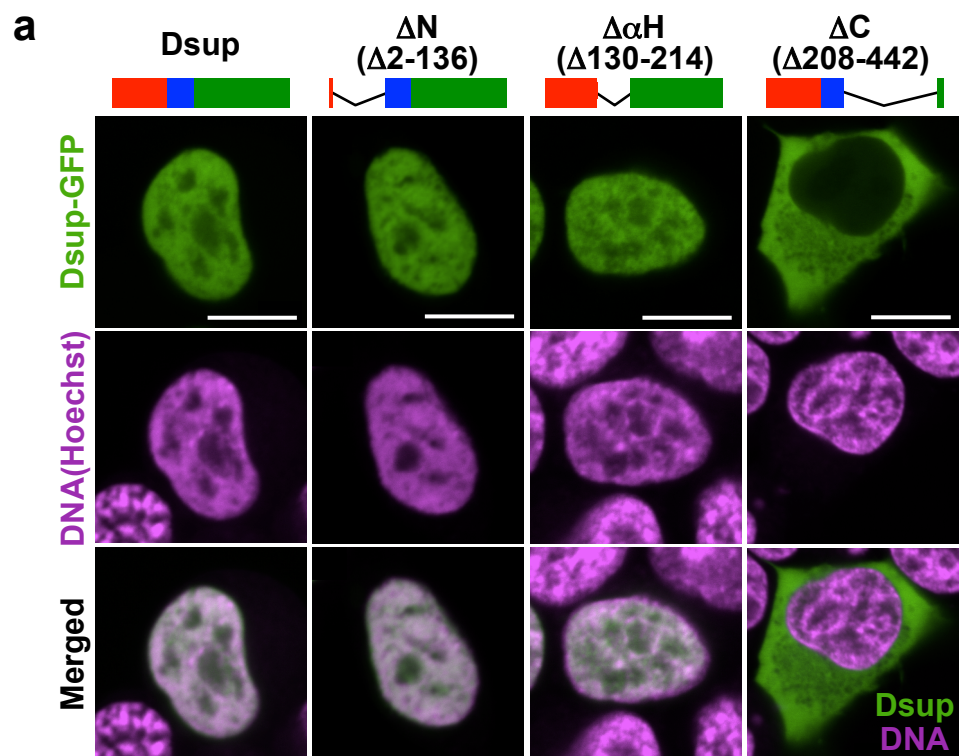


Figure 13. C-Terminal region is responsible for localization to nuclear DNA

(a) Subcellular localization of Dsup-GFP fusion proteins with deletion of the N-terminus (ΔN , $\Delta 2$ -136 aa), α -helical region ($\Delta\alpha H$, $\Delta 130$ -214 aa), and C-terminus (ΔC , $\Delta 208$ -442 aa) in transiently transfected HEK293 cells. Schematic structures are shown above the images. Scale bars, 10 μm . (b) C-terminal region of Dsup protein (Dsup-C) alone is sufficient for localization to nuclear DNA. Closed arrowheads indicate nuclei of Dsup-C-GFP expressing cells and open arrowheads indicate nuclei of non-expressing cells. Dsup-C-GFP expressing cells exhibited aggregated distributions of nuclear DNA. Scale bars, 10 μm . (c) Subcellular localization of Dsup-GFP fusion proteins with Dsup-C deletion derivatives. Schematic structures are shown above the images with the number of remaining amino acids (aa). Scale bars, 10 μm .

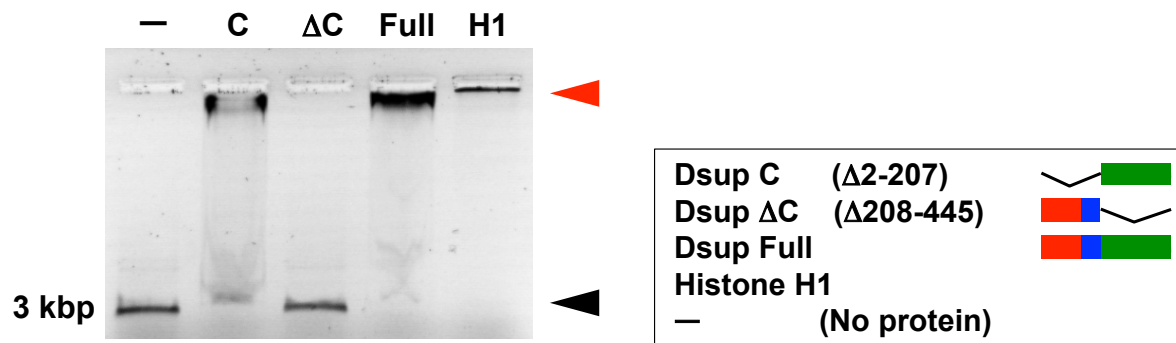


Figure 14. C-Terminal region is responsible for association with DNA *in vitro*

Effect of Dsup protein lacking the C-terminal region on DNA mobility. Black arrowhead indicates the predicted size of the unbound linear probe DNA (3 kbp, 10 ng). Red arrowhead indicates the position of the extremely slowly migrating DNA in the presence of full-length Dsup protein (Full, 100 ng) or C-terminal region alone (C, Δ2-207 aa, 100 ng). The C-terminal region alone was sufficient to shift DNA mobility similar to that of full-length Dsup protein. In contrast, Dsup protein lacking the C-terminal region (ΔC, Δ208-445 aa, 100 ng) completely lost the ability to shift the DNA mobility, suggesting that the C-terminal region is essential for the association with DNA. Histone H1 (H1, 100 ng) was used as a control.

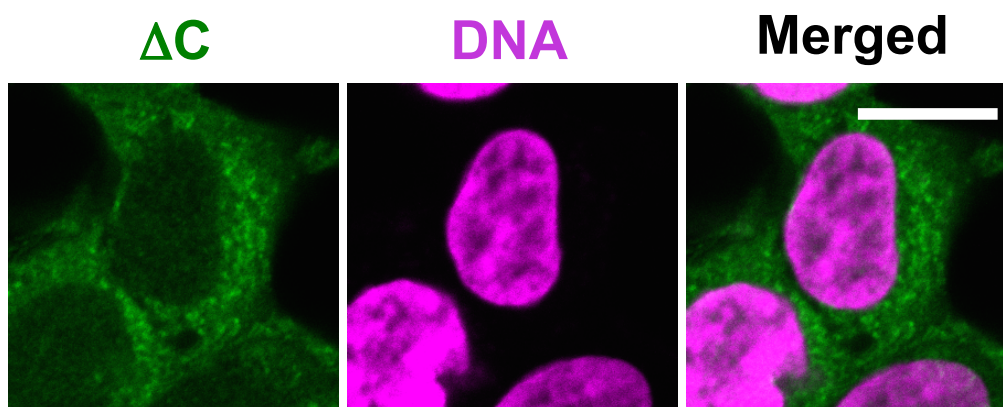


Figure 15. Subcellular localization of Dsup proteins lacking C-terminal DNA-associating region in stably transfected HEK293 cells

Subcellular localization of Dsup proteins lacking C-terminal DNA-associating region (ΔC) were examined by immunocytochemistry in stably transfected HEK293 cells expressing Nuclear DNA was visualized by DAPI staining. Dsup ΔC protein localized mainly in the cytoplasm. Scale bars, 10 μm .

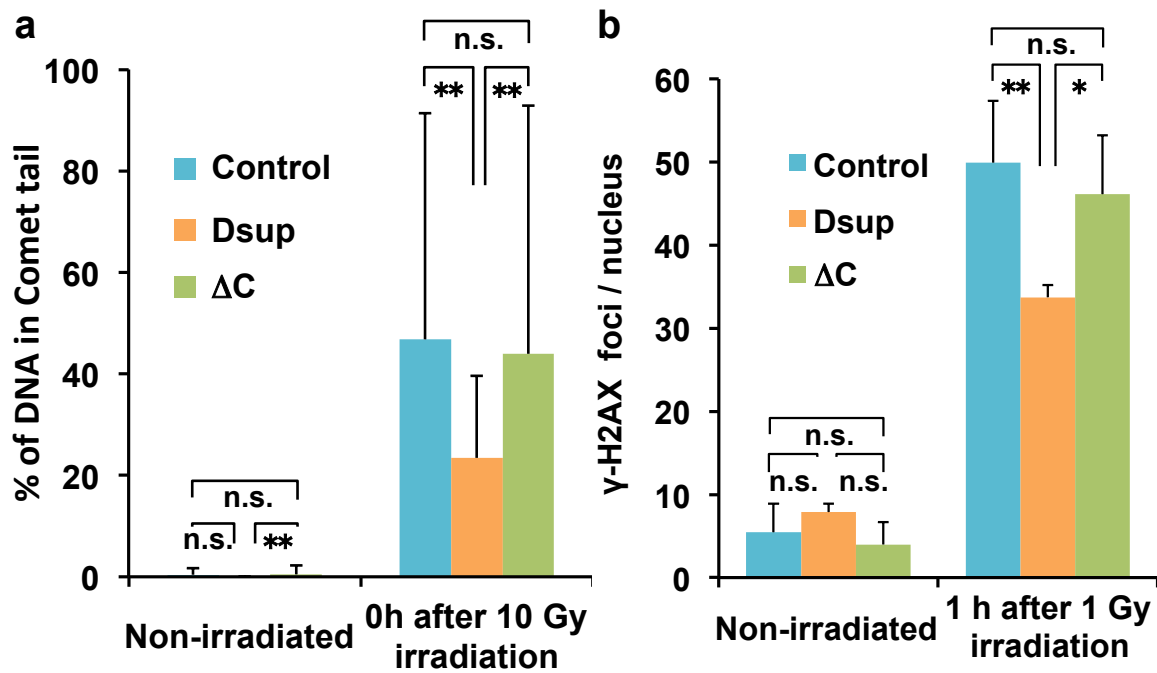


Figure 16. Requirement of the C-terminal region of Dsup protein for DNA protection activity in Dsup-expressing cells

The effects of full-length Dsup and Dsup lacking the C-terminal region (DsupΔC) on DNA breaks caused by X-ray were analyzed using (a) an alkaline comet assay and (b) a γ -H2AX assay. (a) In the alkaline comet assays, DNA fragmentation was assessed as the proportion of DNA detected in the tail region (% of DNA in Comet tail) and compared among untransfected HEK293 cells (Control), full-length Dsup-expressing cells (Dsup) and DsupΔC-expressing cells (ΔC). In contrast to Dsup-expressing cells, which exhibited approximately 50% reduction in the proportion of fragmented DNA, DsupΔC-expressing cells exhibited no reduction compared to control cells. At least 120 comets were analyzed for each condition. Values represent mean \pm s.d., ** P <0.01, n.s. indicates not significant (Tukey-Kramer's test). (b) Quantitative comparison of γ -H2AX foci number under non-irradiated and X-ray irradiated conditions. At least 62 nuclei were analyzed for each condition. Values represent mean \pm s.d.. * P <0.05, ** P <0.01, n.s. indicates not significant (Tukey-Kramer's test).

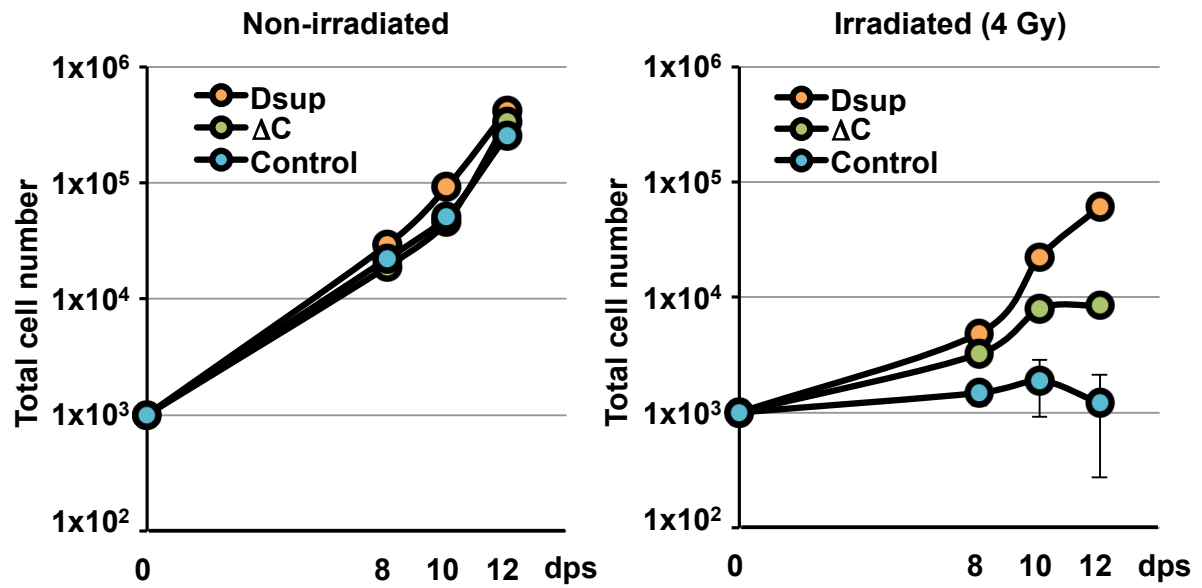


Figure 17. Effect of C-terminal region of Dsup protein on improved cell proliferative ability in irradiated Dsup-expressing cells

Comparison of the cell proliferation curves of parental HEK293 cells (Control), Dsup-expressing cells (Dsup), and DsupΔC-expressing cells (ΔC) under non-irradiated and irradiated conditions. Values represent mean \pm s.d. dps, days post seeding.

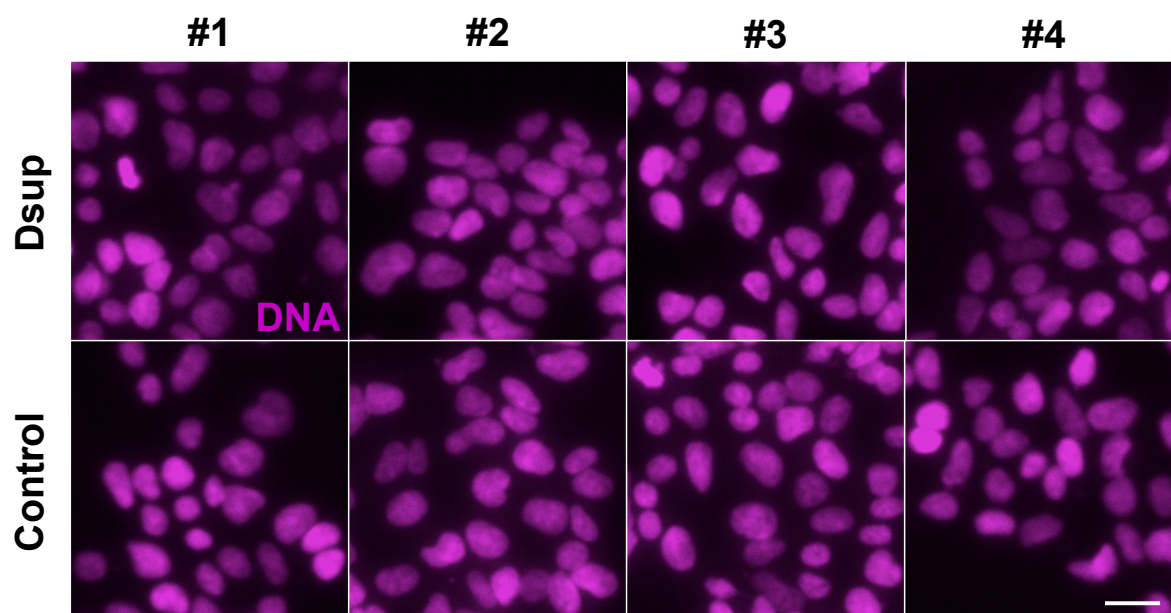


Figure 18. Comparison of the DAPI-stained images between Dsup-expressing cells and control cells

The stable line expressing Dsup (Dsup) and control HEK293 cells (Control) were stained with DAPI after fixation with 4% formaldehyde. No significant difference was observed in distribution of nuclear DNA and fluorescence strength between Dsup-expressing cells and control cells. The fluorescent images were captured using a fluorescent microscope (BZ-9000, Keyence). Each image corresponds to almost the same area in the different wells (#1-4). Scale bar, 20 μm .

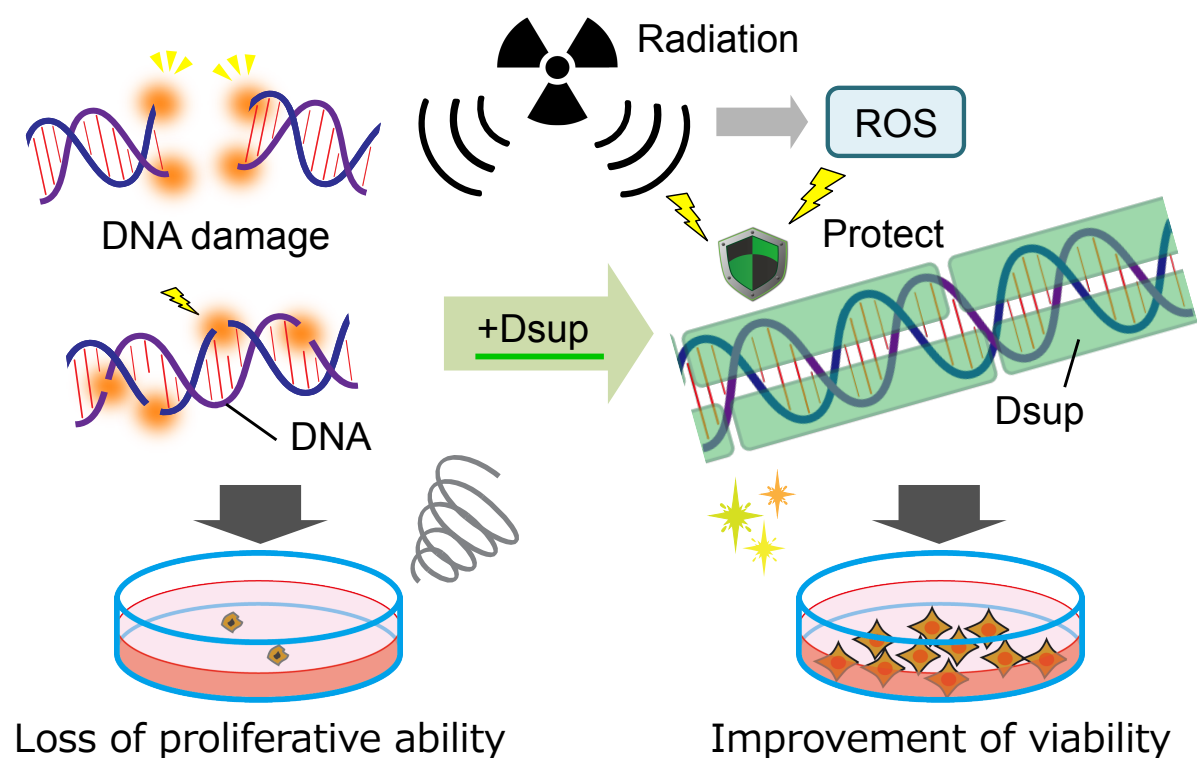
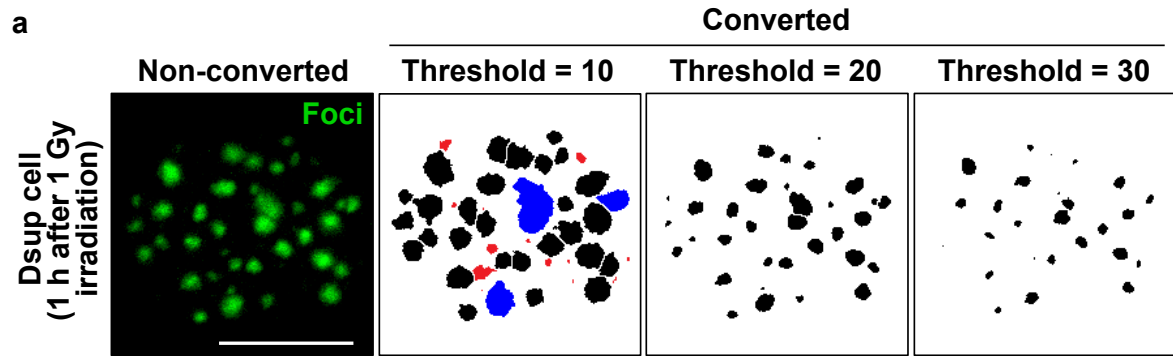


Figure 19. Schematic model of DNA protection by Dsup protein from radiation damage

Radiation induces DNA damage, such as double-strand breaks (DSBs) and single-strand breaks (SSBs), which interfere DNA replication and gene expression. Heavily damaged cells lose their proliferative ability and are destined to death. Dsup protein associated with nuclear DNA could be beneficial to suppress X-ray induced DNA damage through physical shielding or protection from indirect radiation effects (reactive oxygen species, ROS). Thereby, Dsup protein could improve the radio-tolerance of cultured animal cells.



e

Control cells (1 h after 1 Gy irradiation)

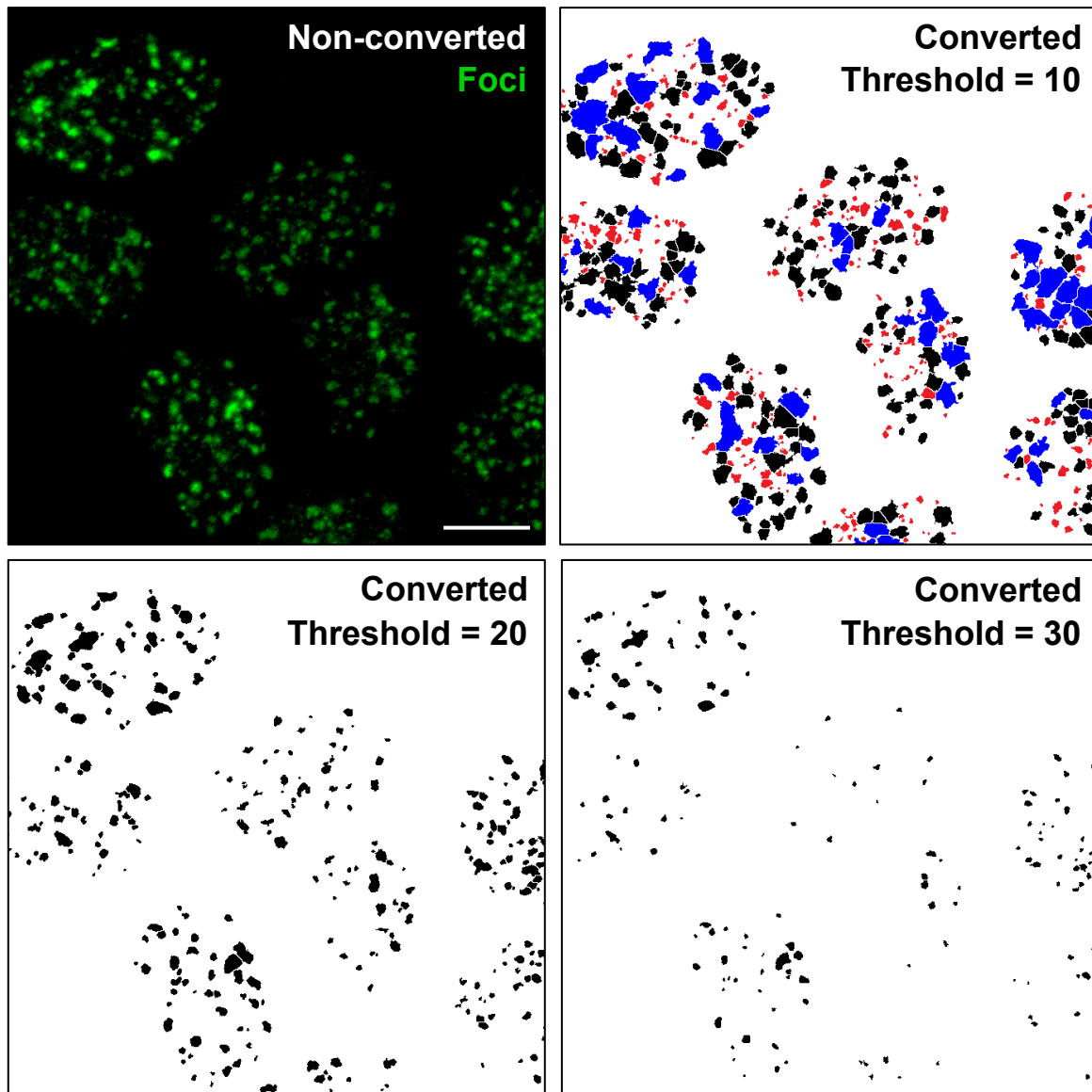


Figure 20. The effect of the image conversion threshold values on visual output and the detection of γ -H2AX foci

The numbers of γ -H2AX foci were counted after conversion of the original fluorescent image to a binarized image. The threshold value for image conversion was manually adjusted, until a visually best fit between the original (non-converted) and converted images of irradiated Dsup cells were observed for each experiment. (a) Representative non-converted fluorescent image and the converted images using the various threshold values of irradiated Dsup-expressing cells. The image converted with the threshold value of 20 produced the best fit to the original fluorescent image. Application of the lower threshold value (10) produced artificial fusions of neighboring foci (shown in blue) and erroneous detections of small dim (background-level) fluorescent signals (shown in red). The threshold value of 30 reduced the foci signals too much. Similar results were observed in irradiated control HEK293 cells (e). Scale bars, 10 μ m. (b) The effect of the threshold values on the mean number of detected γ -H2AX foci per nucleus. Under the irradiated condition, Dsup-expressing cells (Dsup) exhibited a constantly lower number of foci than that in untransfected HEK293 cells (Control) except the occasional case with the threshold value of 2. (c) Quantitative comparison of the foci sizes between control cells and Dsup-expressing cells with various conversion thresholds. With the threshold of 20, the foci size of Dsup-expressing cells is smaller than that of control cells. With the threshold value of 17, enhancing the detection sensitivity, Dsup cells exhibited a distribution of foci sizes similar to that of control cells converted with the threshold of 20. (d) Pairwise statistical analysis of the foci number between Dsup-expressing cells and control cells under irradiated condition. Regardless of whether the same threshold value (20) was used for two cell lines, or more sensitive threshold value (17) was used for Dsup-expressing cells to equalize the foci size distribution between two cell lines, Dsup-expressing cells exhibited statistically significant decrease in foci

number compared to that of control cells (converted with the threshold of 20), robustly confirming that Dsup suppressed DNA breaks.

Tables

Table 1. Statistical measures of DNA fragmentation in the alkaline comet assay

Experimental design	Trial ID	Dose	Cell line	N ^a	% of DNA in Comet tail	
					Mean	s.d.
Control vs. Dsup vs. DsupΔC	#1	0 Gy	Control	302	0.25	3.6
			Dsup	323	1.0	2.1
			ΔC	252	0.94	1.7
		10 Gy	Control	281	33.8	32.7
			Dsup	295	16.1	9.7
			ΔC	298	37.2	25.4
	#2	0 Gy	Control	170	0.41	1.4
			Dsup	173	0.017	0.085
			ΔC	120	0.47	1.8
		10 Gy	Control	179	46.8	44.6
			Dsup	202	23.4	16.2
			ΔC	127	44.0	49.0

^a The number of analyzed comets in each condition.

Table 2. Statistical test of the effect of Dsup on DNA fragmentation in the alkaline comet assay

Experimental design	Trial ID	Dose	Comparison pair	<i>p</i> -value (Tukey-Kramer's test)	Significance ^a
Control vs. Dsup vs. DsupΔC	#1	0 Gy	Control vs. Dsup	9.2E-05	***
			Control vs. ΔC	0.0062	**
			Dsup vs. ΔC	0.94	n.s.
		10 Gy	Control vs. Dsup	7.5E-13	***
			Control vs. ΔC	0.22	n.s.
			Dsup vs. ΔC	7.5E-13	***
	#2	0 Gy	Control vs. Dsup	0.99	n.s.
			Control vs. ΔC	0.53	n.s.
			Dsup vs. ΔC	0.31	n.s.
		10 Gy	Control vs. Dsup	1.6E-10	***
			Control vs. ΔC	0.79	n.s.
			Dsup vs. ΔC	1.7E-10	***

^a *** $P < 0.01$, *** $P < 0.001$, n.s. indicates not significant

Table 3. Statistical measures of DNA damage induced by H₂O₂ in the alkaline comet assay

Experimental design	Trial ID	Cell line	H ₂ O ₂ (100 µM)	NAC (10 mM)	N ^a	% of DNA in Comet tail	
						Mean	s.d.
Control vs. Dsup	#1	Control	-	-	415	2.8	5.5
			+	-	356	70.6	26.1
			+	+	445	47.4	30.3
			-	+	344	1.8	2.9
	Dsup		-	-	320	2.5	6.1
			+	-	540	17.7	12.6
			+	+	534	11.9	10.1
			-	+	346	2.2	3.1
#2	Control		-	-	423	4.1	5.0
			+	-	306	64.3	31.7
			+	+	331	33.8	32.4
			-	+	302	2.9	4.1
	Dsup		-	-	423	3.5	6.5
			+	-	379	18.0	15.6
			+	+	371	11.0	8.3
			-	+	347	2.0	2.7

^a The number of analyzed comets in each condition.

Table 4. Statistical test of the effect of Dsup on damage induced by H₂O₂ in the alkaline comet assay

Experimental design	Trial ID	Comparison pair	p-value (Tukey-Kramer's test)	Significance ^a
Control vs. Dsup	#1	Control vs. Control+H ₂ O ₂	<1.0E-15	***
		Control vs. Control+H ₂ O ₂ +NAC	<1.0E-15	***
		Control vs. Control+NAC	0.99	n.s.
		Control vs. Dsup	0.99	n.s.
		Control vs. Dsup+H ₂ O ₂	<1.0E-15	***
		Control vs. Dsup+H ₂ O ₂ +NAC	<1.0E-15	***
		Control vs. Dsup+NAC	0.99	n.s.
		Control+H ₂ O ₂ vs. Control+H ₂ O ₂ +NAC	<1.0E-15	***
		Control+H ₂ O ₂ vs. Control+NAC	<1.0E-15	***
		Control+H ₂ O ₂ vs. Dsup	<1.0E-15	***
		Control+H ₂ O ₂ vs. Dsup+H ₂ O ₂	<1.0E-15	***
		Control+H ₂ O ₂ vs. Dsup+H ₂ O ₂ +NAC	<1.0E-15	***
		Control+H ₂ O ₂ vs. Dsup+NAC	<1.0E-15	***
		Control+H ₂ O ₂ +NAC vs. Control+NAC	<1.0E-15	***
		Control+H ₂ O ₂ +NAC vs. Dsup	<1.0E-15	***
		Control+H ₂ O ₂ +NAC vs. Dsup+H ₂ O ₂	<1.0E-15	***
		Control+H ₂ O ₂ +NAC vs. Dsup+H ₂ O ₂ +NAC	<1.0E-15	***
		Control+H ₂ O ₂ +NAC vs. Dsup+NAC	<1.0E-15	***
		Control+NAC vs. Dsup	0.99	n.s.
		Control+NAC vs. Dsup+H ₂ O ₂	<1.0E-15	***
		Control+NAC vs. Dsup+H ₂ O ₂ +NAC	<1.0E-15	***
		Control+NAC vs. Dsup+NAC	0.99	n.s.
		Dsup vs. Dsup+H ₂ O ₂	<1.0E-15	***
		Dsup vs. Dsup+H ₂ O ₂ +NAC	<1.0E-15	***
		Dsup vs. Dsup+NAC	0.99	n.s.
		Dsup+H ₂ O ₂ vs. Dsup+H ₂ O ₂ +NAC	2.86E-08	***
		Dsup+H ₂ O ₂ vs. Dsup+NAC	<1.0E-15	***
		Dsup+H ₂ O ₂ +NAC vs. Dsup+NAC	<1.0E-15	***
	#2	Control vs. Control+H ₂ O ₂	<1.0E-15	***
		Control vs. Control+H ₂ O ₂ +NAC	<1.0E-15	***
		Control vs. Control+NAC	0.98	n.s.
		Control vs. Dsup	0.99	n.s.
		Control vs. Dsup+H ₂ O ₂	<1.0E-15	***
		Control vs. Dsup+H ₂ O ₂ +NAC	9.45E-07	***
		Control vs. Dsup+NAC	0.66	n.s.
		Control+H ₂ O ₂ vs. Control+H ₂ O ₂ +NAC	<1.0E-15	***
		Control+H ₂ O ₂ vs. Control+NAC	<1.0E-15	***
		Control+H ₂ O ₂ vs. Dsup	<1.0E-15	***
		Control+H ₂ O ₂ vs. Dsup+H ₂ O ₂	<1.0E-15	***
		Control+H ₂ O ₂ vs. Dsup+H ₂ O ₂ +NAC	<1.0E-15	***
		Control+H ₂ O ₂ vs. Dsup+NAC	<1.0E-15	***
		Control+H ₂ O ₂ +NAC vs. Control+NAC	<1.0E-15	***
		Control+H ₂ O ₂ +NAC vs. Dsup	<1.0E-15	***
		Control+H ₂ O ₂ +NAC vs. Dsup+H ₂ O ₂	<1.0E-15	***
		Control+H ₂ O ₂ +NAC vs. Dsup+H ₂ O ₂ +NAC	<1.0E-15	***
		Control+H ₂ O ₂ +NAC vs. Dsup+NAC	<1.0E-15	***
		Control+NAC vs. Dsup	0.99	n.s.
		Control+NAC vs. Dsup+H ₂ O ₂	<1.0E-15	***
		Control+NAC vs. Dsup+H ₂ O ₂ +NAC	5.54E-08	***
		Control+NAC vs. Dsup+NAC	0.99	n.s.
		Dsup vs. Dsup+H ₂ O ₂	<1.0E-15	***
		Dsup vs. Dsup+H ₂ O ₂ +NAC	2.1E-08	***
		Dsup vs. Dsup+NAC	0.95	n.s.
		Dsup+H ₂ O ₂ vs. Dsup+H ₂ O ₂ +NAC	2.3E-08	***
		Dsup+H ₂ O ₂ vs. Dsup+NAC	<1.0E-15	***
		Dsup+H ₂ O ₂ +NAC vs. Dsup+NAC	1.23E-10	***

^a ****P*<0.001, n.s. indicates not significant

Table 5. Statistical measures of DNA fragmentation in the neutral comet assay

Experimental design	Trial ID	Dose	Cell line	N ^a	% of DNA in Comet tail	
					Mean	s.d.
Control vs. Dsup	#1	0 Gy	Control	300	7.5	8.7
			Dsup	300	5.8	6.5
		5 Gy	Control	300	35.5	26.3
			Dsup	300	21.1	21.0
	#2	0 Gy	Control	300	11.7	6.7
			Dsup	300	13.0	6.8
		5 Gy	Control	300	30.5	10.2
			Dsup	300	20.4	9.7
	#3	0 Gy	Control	300	9.6	11.9
			Dsup	300	10.9	7.0
		5 Gy	Control	300	32.7	12.1
			Dsup	300	19.0	10.0

^a The number of analyzed comets in each condition.

Table 6. Pairwise statistical test of the effect of Dsup on DNA fragmentation in the neutral comet assay

Pairwise comparison	Trial ID	Dose	p-value (F-test) ^a	Statistical method	t-value	p-value	Significance ^b
Control vs. Dsup	#1	0 Gy	7.8E-07	Welch's t-test	2.758	0.0060	**
		5 Gy	8.9E-05	Welch's t-test	7.406	4.7E-13	***
	#2	0 Gy	8.8E-01	Student's t-test	-2.266	0.024	*
		5 Gy	3.4E-01	Student's t-test	6.263	7.2E-10	***
	#3	0 Gy	2.8E-18	Welch's t-test	-1.541	0.12	n.s.
		5 Gy	6.0E-04	Welch's t-test	15.099	<1.0E-15	***

^a Equality of variances was tested using F-test (significance level = 0.05).

^b * $P < 0.05$, ** $P < 0.01$, *** $P < 0.001$, n.s. indicates not significant

Table 7. Statistical data regarding the number of foci in the γ -H2AX assay

Experimental design	Trial ID	Dose	Cell line	N ^a	The number of foci / nucleus	
					Mean	s.d.
Control vs. Dsup	#1	0 Gy	Control	52	11.0	13.7
			Dsup	73	6.8	8.9
		1 Gy	Control	53	38.4	15.0
			Dsup	71	22.8	11.8
Control vs. Dsup vs. Dsup+shDsup	#1	0 Gy	Control	77	3.2	1.9
			Dsup	74	5.2	2.0
			Dsup+shDsup	70	3.2	1.2
		1 Gy	Control	70	40.1	9.1
			Dsup	92	26.6	5.2
			Dsup+shDsup	74	42.1	5.9
	#2	0 Gy	Control	40	3.8	4.2
			Dsup	35	5.9	3.4
			Dsup+shDsup	40	4.8	3.8
		1 Gy	Control	36	38.5	5.2
			Dsup	54	28.0	2.1
			Dsup+shDsup	40	38.4	4.4
Control vs. Dsup vs. Dsup Δ C	#1	0 Gy	Control	59	0.19	0.58
			Dsup	63	1.0	0.22
			Δ C	62	0.32	0.27
		1 Gy	Control	59	28.4	5.1
			Dsup	74	14.8	6.4
			Δ C	60	22.2	7.5
	#2	0 Gy	Control	77	5.4	3.4
			Dsup	65	7.9	1.0
			Δ C	62	3.9	2.7
		1 Gy	Control	75	50.6	7.5
			Dsup	64	33.8	1.5
			Δ C	73	46.7	7.1

^a The number of analyzed nuclei in each condition.

Table 8. Pairwise statistical test of the effect of Dsup on the number of foci in the γ -H2AX assay

Pairwise comparison	Trial ID	Dose	p-value (F-test) ^a	Statistical method	t-value	p-value	Significance ^b
Control vs. Dsup	#1	0 Gy	7.84.E-04	Welch's t-test	1.962	0.052	n.s.
		1 Gy	5.90.E-02	Welch's t-test	6.489	3.8E-09	***

^a Equality of variances was tested using F-test (significance level = 0.05).

^b *** $P < 0.001$, n.s. indicates not significant

Table 9. Statistical analysis of the effect of Dsup on the number of foci in the γ -H2AX assay

Experimental design	Trial ID	Dose	Comparison pair	<i>p</i> -value (Tukey-Kramer's test)	Significance ^a
Control vs. Dsup vs. Dsup+shDsup	#1	0 Gy	Control vs. Dsup	0.15	n.s.
			Control vs. Dsup+shDsup	1.0	n.s.
			Dsup vs. Dsup+shDsup	0.15	n.s.
	1 Gy		Control vs. Dsup	0.0023	**
			Control vs. Dsup+shDsup	0.92	n.s.
			Dsup vs. Dsup+shDsup	8.9E-04	***
	#2	0 Gy	Control vs. Dsup	0.70	n.s.
			Control vs. Dsup+shDsup	0.90	n.s.
			Dsup vs. Dsup+shDsup	0.89	n.s.
	1 Gy		Control vs. Dsup	0.0094	**
			Control vs. Dsup+shDsup	1.0	n.s.
			Dsup vs. Dsup+shDsup	0.0036	**
Control vs. Dsup vs. DsupΔC	#1	0 Gy	Control vs. Dsup	0.38	n.s.
			Control vs. ΔC	0.69	n.s.
			Dsup vs. ΔC	0.14	n.s.
	1 Gy		Control vs. Dsup	0.0039	**
			Control vs. ΔC	0.57	n.s.
			Dsup vs. ΔC	0.027	*
	#2	0 Gy	Control vs. Dsup	0.018	*
			Control vs. ΔC	0.89	n.s.
			Dsup vs. ΔC	0.047	*
	1 Gy		Control vs. Dsup	0.0022	**
			Control vs. ΔC	0.14	n.s.
			Dsup vs. ΔC	0.17	n.s.

^a * $P < 0.05$, ** $P < 0.01$, *** $P < 0.001$, n.s. indicates not significant

Table 10. Effect of Dsup on the cell number over time

Experimental design	Trial ID	Dose	Cell line	N	8 dps		10 dps		12 dps	
					Mean ^a	s.d. ^a	Mean ^a	s.d. ^a	Mean ^a	s.d. ^a
Control vs. Dsup vs. Dsup+shDsup	#1	0 Gy	Control	3	44,502	9,694	117,649	37,205	179,154	23,127
			Dsup	3	219,804	60,518	618,684	37,335	733,030	78,866
			Dsup+shDsup	3	24,725	3,778	75,734	29,838	182,584	10,981
		4 Gy	Control	3	1,264	484	931	74	343	388
			Dsup	3	5,772	812	18,914	6,556	82,487	27,745
			Dsup+shDsup	3	1,441	473	1,686	450	882	574
	#2	0 Gy	Control	3	19,963	3,602	43,218	6,285	165,992	32,313
			Dsup	3	151,273	33,213	600,975	54,620	826,914	53,068
			Dsup+shDsup	3	42,463	13,143	114,895	60,949	193,981	54,863
		4 Gy	Control	3	1,392	309	8,840	4,164	539	279
Control vs. Dsup vs. DsupΔC	#1	0 Gy	Dsup	3	3,440	841	1,166	767	54,606	7,044
			Dsup+shDsup	3	1,156	456	1,245	1,095	510	139
			ΔC	3	18,840	2,143	46,433	7,335	335,071	20,356
		4 Gy	Control	3	1,481	584	1,899	1,698	1,205	1,615
			Dsup	3	4,888	1,603	22,261	2,485	60,627	5,739
			ΔC	3	3,232	450	7,979	1,296	8,470	2,583
	#2	0 Gy	Control	3	42,555	9,085	106,635	13,435	646,104	51,957
			Dsup	3	58,445	22,937	188,612	4,595	985,464	171,824
			ΔC	3	46,931	3,498	138,450	18,236	756,584	28,496
		4 Gy	Control	3	4,134	790	8,262	2,308	8,471	3,336
Control vs. Dsup vs. DsupΔC	#1	0 Gy	Dsup	3	9,211	2,359	24,179	5,348	63,105	14,288
			ΔC	3	6,801	993	13,069	3,455	17,922	6,023
	#2	0 Gy	Control	3	42,555	9,085	106,635	13,435	646,104	51,957
			Dsup	3	58,445	22,937	188,612	4,595	985,464	171,824
			ΔC	3	46,931	3,498	138,450	18,236	756,584	28,496
		4 Gy	Control	3	4,134	790	8,262	2,308	8,471	3,336
			Dsup	3	9,211	2,359	24,179	5,348	63,105	14,288
			ΔC	3	6,801	993	13,069	3,455	17,922	6,023
	#2	0 Gy	Control	3	42,555	9,085	106,635	13,435	646,104	51,957
			Dsup	3	58,445	22,937	188,612	4,595	985,464	171,824
			ΔC	3	46,931	3,498	138,450	18,236	756,584	28,496

^a Mean and standard deviation (s.d.) values are shown for the cell number at each point.

dps; days post seeding

References

- Almiron, M. Link, A. J. Furlong, D. & Kolter, R. A novel DNA-binding protein with regulatory and protective roles in starved *Escherichia coli*. *Genes Dev.* **6**, 2646–2654 (1992).
- Andrievski, A. & Wilkins, R. C. The response of gamma-H2AX in human lymphocytes and lymphocytes subsets measured in whole blood cultures. *Int. J. Radiat. Biol.* **85**, 369–376 (2009).
- Battista, J. R. Against all odds: the survival strategies of *Deinococcus radiodurans*. *Annu. Rev. Microbiol.* **51**, 203–224 (1997).
- Biaglow, J. E. The effects of ionizing radiation on mammalian cells. *J. Chem. Educ.* **58**, 144–156 (1981).
- Burg, M. Van Der, Veelen, L. R. Van, Verkaik, N. S., Wiegant, W. W., Hartwig, N. G., Barendregt, B. H., Brugmans, L., Raams, A., Jaspers, N. G. J., Zdzienicka, M. Z., Dongen, J. J. M. Van & Gent, D. C. Van. A new type of radiosensitive T-B –NK+ severe combined immunodeficiency caused by a LIG4 mutation. *J. Clin. Invest.* **116**, 137–145 (2006).
- Cai, Z., Vallis, K. A. & Reilly, R. M. Computational analysis of the number, area and density of γ -H2AX foci in breast cancer cells exposed to ^{111}In -DTPA-hEGF or γ -rays using Image-J software. *Int. J. Radiat. Biol.* **85**, 262–271 (2009).

Cucinotta, F. A. *et al.* How safe is safe enough? Radiation risk for a human mission to Mars. *PLoS One* **8**, e74988 (2013).

Chapman, J. R. Taylor, M. R. & Boulton, S. J. Playing the end game: DNA double-strand break repair pathway choice. *Mol. Cell* **47**, 497–510 (2012).

Ciccia, A. & Elledge, S. J. The DNA damage response: making it safe to play with knives. *Mol. Cell* **40**, 179–204 (2010).

Emanuelsson, O., Nielsen, H., Brunak, S. & von Heijne, G. Predicting subcellular localization of proteins based on their N-terminal amino acid sequence. *J. Mol. Biol.* **300**, 1005–1016 (2000).

França, M. B., Panek, A. D. & Eleutherio, E. C. A. Oxidative stress and its effects during dehydration. *Comp. Biochem. Physiol.* **146**, 621–31 (2007).

Frenkiel-Krispin, D., Levin-Zaidman, S., Shimoni, E., Wolf, S. G., Wachtel, E. J., Arad, T., Finkel, S. E., Kolter, R. & Minsky, A. Regulated phase transitions of bacterial chromatin: a non-enzymatic pathway for generic DNA protection. *EMBO J.* **20**, 1184–1191 (2001).

Gladyshev, E. & Meselson, M. Extreme resistance of bdelloid rotifers to ionizing radiation. *Proc. Natl. Acad. Sci. USA* **105**, 5139–5144 (2008).

Gusev, O., Nakahara, Y., Vanyagina, V., Malutina, L., Cornette, R., Sakashita, T., Hamada, N., Kikawada, T., Kobayashi, Y. & Okuda, T. Anhydrobiosis-associated nuclear DNA

damage and repair in the sleeping chironomid: linkage with radioresistance. *PLoS ONE* **5**, e14008 (2010).

Hashimoto, T., Horikawa, D. D., Saito, Y., Kuwahara, H., Kozuka-Hata, H., Shin-I, T., Minakuchi, Y., Ohishi, K., Motoyama, A., Aizu, T., Enomoto, A., Kondo, K., Tanaka, S., Hara, Y., Koshikawa, S., Sagara, H., Miura, T., Yokobori, S., Miyagawa, K., Suzuki, Y., Kubo, T., Oyama, M., Kohara, Y., Fujiyama, A., Arakawa, K., Katayama, T., Toyoda, A. & Kunieda, T. Extremotolerant tardigrade genome and improved radiotolerance of human cultured cells by tardigrade-unique protein. *Nat. Commun.* in press.

Hespeels, B., Knapen, M., Hanot-Mambres, D., Heuskin, A. C., Pineux, F., Lucas, S., Koszul, R. & Van Doninck, K. Gateway to genetic exchange? DNA double-strand breaks in the bdelloid rotifer *Adineta vaga* submitted to desiccation. *J. Evol. Biol.* **27**, 1334-1345 (2014).

Horikawa, D. D., Kunieda, T., Abe, W., Watanabe, M., Nakahara, Y., Yukuhiro, F., Sakashita, T., Hamada, N., Wada, S., Funayama, T., Katagiri, C., Kobayashi, Y., Higashi, S. & Okuda, T. Establishment of a rearing system of the extremotolerant tardigrade *Ramazzottius varieornatus*: a new model animal for astrobiology. *Astrobiology* **8**, 549–556 (2008).

Horikawa, D. D., Sakashita, T., Katagiri, C., Watanabe, M., Kikawada, T., Nakahara, Y., Hamada, N., Wada, S., Funayama, T., Higashi, S., Kobayashi, Y., Okuda, T. & Kuwabara, M. Radiation tolerance in the tardigrade *Milnesium tardigradum*. *Int. J. Radiat. Biol.* **82**, 843–848 (2006).

Horikawa, D. D., Yamaguchi, A., Sakashita, T., Tanaka, D., Hamada, N., Yukuhiro, F., Kuwahara, H., Kunieda, T., Watanabe, M., Nakahara, Y., Wada, S., Funayama, T., Katagiri, C., Higashi, S., Yokobori, S-I., Kuwabara, M., Rothschild, L. J., Okuda, T., Hashimoto, H. & Kobayashi, Y. Tolerance of anhydrobiotic eggs of the Tardigrade *Ramazzottius varieornatus* to extreme environments. *Astrobiology* **12**, 283–289 (2012).

Horton, P., Park, K. J., Obayashi, T., Fujita, N., Harada, H., Adams-Collier, C. J. & Nakai, K. WoLF PSORT: protein localization predictor. *Nucleic Acids Res.* **35**, W585–W587 (2007).

Jackson, S. P. Sensing and repairing DNA double-strand breaks. *Carcinogenesis* **23**, 687–696 (2002).

Jackson, S. P. & Bartek, J. The DNA-damage response in human biology and disease. *Nature* **461**, 1071–1078 (2009).

John, E. B. The effects of ionizing radiation on mammalian cells. *J. Chem. Educ.* **58**, 144–156 (1981).

Jönsson, K. I., Rabbow, E., Schill, R. O., Harms-Ringdahl, M. & Rettberg, P. Tardigrades survive exposure to space in low Earth orbit. *Curr. Biol.* **18**, R729–R731 (2008).

Kegel, P., Riballo, E., Kühne, M., Jeggo, P. A. & Löbrich, M. X-irradiation of cells on glass slides has a dose doubling impact. *DNA Repair.* **6**, 1692–1697 (2007).

Kitta, K., Day, R. M., Ikeda, T. & Suzuki, Y. J. Hepatocyte growth factor protects cardiac

myocytes against oxidative stress-induced apoptosis. *Free Radic. Biol. Med.* **31**, 902–910 (2001).

Końca, K., Lankoff, A., Banasik, A., Lisowska, H., Kuszewski, T., Stanisław, G., Koza, Z. & Wojcik, A. A cross-platform public domain PC image-analysis program for the comet assay. *Mutat. Res.* **534**, 15–20 (2003).

Krisko, A., Leroy, M., Radman, M. & Meselson, M. Extreme anti-oxidant protection against ionizing radiation in bdelloid rotifers. *Proc. Natl. Acad. Sci. USA* **109**, 2354–2357 (2012).

Kyte, J. & Doolittle, R. F. A simple method for displaying the hydropathic character of a protein. *J. Mol. Biol.* **157**, 105–132 (1982).

Martinez, A. & Kolter, R. Protection of DNA during oxidative stress by the nonspecific DNA-binding protein Dps. *J. Bacteriol.* **179**, 5188–5194 (1997).

Mattimore, V. & Battista, J. Radioresistance of *Deinococcus radiodurans*: functions necessary to survive ionizing radiation are also necessary to survive prolonged desiccation. *J. Bacteriol.* **178**, 633–637 (1996).

Naito, Y., Yoshimura, J., Morishita, S. & Ui-Tei, K. siDirect 2.0: updated software for designing functional siRNA with reduced seed-dependent off-target effect. *BMC Bioinformatics* **10**, 392 (2009).

Nassour, J., Martien, S., Martin, N., Deruy, E., Tomellini, E., Malaquin, N., Bouali, F.,

Sabatier, L., Wernert, N., Pinte, S., Gilson, E., Pourtier, A., Pluquet, O. & Abbadie, C. Defective DNA single-strand break repair is responsible for senescence and neoplastic escape of epithelial cells. *Nat. Commun.* **7**, 10399 (2016).

Neumann, S. Reuner, A. Brümmer, F & Schill, R. O. DNA damage in storage cells of anhydrobiotic tardigrades. *Comp. Biochem. Physiol. A* **153**, 425–429 (2009).

Niwa, H., Yamamura, K. & Miyazaki, J. Efficient selection for high-expression transfectants with a novel eukaryotic vector. *Gene* **108**, 193–199 (1991).

Noda, A., Hirai, Y., Hamasaki, K., Mitani, H., Nakamura, N. & Kodama, Y. Unrepairable DNA double-strand breaks that are generated by ionising radiation determine the fate of normal human cells. *J. Cell. Sci.* **125**, 5280–5287 (2012).

Puck, T. T. & Marcus, P. I. Action of x-rays on mammalian cells. *J. Exp. Med.* **103**, 653–666 (1956).

Ramløv, H. & Westh, P. Cryptobiosis in the eutardigrade *Adorybiotus (Richtersius) coronifer*: Tolerance to alcohols, temperature and de novo protein synthesis. *Zool. Anz.* **240**, 517–523 (2001).

Rebecchi, L. Cesari, M. Altiero, T. Frigieri, A. & Guidetti, R. Survival and DNA degradation in anhydrobiotic tardigrades. *J. Exp. Biol.* **212**, 4033–4039 (2009).

Rice, P., Longden, I. & Bleasby, A. EMBOSS: The European Molecular Biology Open

Software Suite. *Trends Genet.* **16**, 276–277 (2000).

Rothkamm, K. & Löbrich, M. Evidence for a lack of DNA double-strand break repair in human cells exposed to very low x-ray doses. *Proc. Natl. Acad. Sci. USA* **100**, 5057–5062 (2003).

Setlow, B. Hand, A. R. & Setlow, P. Synthesis of a *Bacillus subtilis* small, acid-soluble spore protein in *Escherichia coli* causes cell DNA to assume some characteristics of spore DNA. *J. Bacteriol.* **173**, 1642–1653 (1991).

Sinclair, W. & Morton, R. X-ray sensitivity during the cell generation cycle of cultured Chinese hamster cells. *Radiat. Res.* **29**, 450–474 (1966).

Slade, D. & Radman, M. Oxidative stress resistance in *Deinococcus radiodurans*. *Microbiol. Mol. Biol. Rev.* **75**, 133–191 (2011).

Spurio, R., Dürrenberger, M., Falconi, M., La Teana, A., Pon, C. L. & Gualerzi, C. O. Lethal overproduction of the *Escherichia coli* nucleoid protein H-NS: ultramicroscopic and molecular autopsy. *Mol. Gen. Genet.* **231**, 201–211 (1992).

Stewart, S. A., Dykxhoorn, D. M., Palliser, D., Mizuno, H., Yu, E. Y., An, D. S., Sabatini, D. M., Chen, I. S. Y., Hahn, W. C., Sharp, P. A., Weinberg, R. A. & Novina, C. D. Lentivirus-delivered stable gene silencing by RNAi in primary cells Lentivirus-delivered stable gene silencing by RNAi in primary cells. *RNA* **9**, 493–501 (2003).

Tanaka, S., Tanaka, J., Miwa, Y., Horikawa, D. D., Katayama, T., Arakawa, K., Toyoda, A., Kubo, T. & Kunieda, T. Novel mitochondria-targeted heat-soluble proteins identified in the anhydrobiotic tardigrade improve osmotic tolerance of human cells. *PLoS One* **10**, e0118272 (2015).

Taneja, N., Davis, M., Choy, J. S., Beckett, M. A., Singh, R., Kron, S. J. & Weichselbaum, R. R. Histone H2AX phosphorylation as a predictor of radiosensitivity and target for radiotherapy. *J. Biol. Chem.* **279**, 2273–2280 (2004).

Tenlen, J. R., McCaskill, S. & Goldstein, B. RNA interference can be used to disrupt gene function in tardigrades. *Dev. Genes Evol.* **223**, 171–181 (2012).

Ward, J. F. DNA damage as the cause of ionizing radiation-induced gene activation. *Radiat. Res.* **138**, S85–88 (1994).

Xu, M., McCanna, D. J. & Sivak, J. G. Use of the viability reagent PrestoBlue in comparison with alamarBlue and MTT to assess the viability of human corneal epithelial cells. *J. Pharmacol. Toxicol. Methods* **71**, 1–7 (2014).

Zahradka, K., Slade, D., Bailone, A., Sommer, S., Averbek, D., Petranovic, M., Lindner, A. B. & Radman, M. Reassembly of shattered chromosomes in *Deinococcus radiodurans*. *Nature* **443**, 569–573 (2006).

Acknowledgements

I would like to give deepest gratitude to Professor Takeo Kubo for providing me the opportunity to enjoy biological sciences and valuable comments. I also express my deepest gratitude to Dr. Takekazu Kunieda for carefully considered training and encouraging me through my master and doctoral course studies.

I sincerely thank my research collaborators, Professor Kiyoshi Miyagawa and Dr. Atsushi Enomoto, for providing opportunity to use the X-ray generator and valuable discussion on interpretation of the results in radiation analyses; Professor Hiroshi Mitani and Dr. Yoshikazu Kuwahara kindly provided valuable suggestions regarding the methods of comet assay and γ -H2AX assay; I also appreciate the helpful assistance of Ms. Yumiko Ishii in flow cytometry analysis.

I am grateful to lab members for their precious suggestions and important discussions during the course of my graduate school research.

Finally, I would like to express my grateful feelings to my family who always kindly supports me.